

Article

Ultrastructural Evidence Elucidates the Mode of Action of Sulfur in Preventing Pollen Tube Development in Stigma of *Citrus* cv. Nadorcott and Other Horticultural Species

Francisco García-Breijo ¹, José Reig ², Nuria Cebrián ¹, Alfonso Garmendia ³, Roberto Beltrán ¹, Carlos Zornoza ⁴ and Hugo Merle ^{1,*}

- ¹ Departamento de Ecosistemas Agroforestales, Universitat Politècnica de València, 46022 Valencia, Spain; fgarcia@eaf.upv.es (F.G.-B.); nucego@hotmail.com (N.C.); robelmar@upvnet.upv.es (R.B.)
- ² Instituto Cavanilles de Biodiversidad y Biología Evolutiva, Universidad de Valencia, 46010 Valencia, Spain; jose.reig@uv.es
- ³ Instituto Agroforestal Mediterráneo, Universitat Politècnica de València, 46022 Valencia, Spain; algarsal@upvnet.upv.es
- ⁴ S.A. Explotaciones Agrícolas Serrano (SAEAS), C/ En Sanz 5-1, 46001 Valencia, Spain; czornoza@saeas.es
- * Correspondence: humerfa@upvnet.upv.es

Abstract: *Citrus* species have a “wet”-type stigma with abundant exudate, and their style contains numerous canals. For successful seed formation, the process includes pollen grain germination on the stigma, pollen tube development and growth through the stigma and style and, ultimately, successful ovule fertilization. However, preventing the fertilization process can be useful for many agronomic and plant-breeding purposes, such as seedless fruits or for developing new varieties. Several studies have recently shown the inhibition effect of sulfur on pollen tube development inside the Nadorcott mandarin stigma and its effective application to obtain seedless mandarins. However, when applied to the stigma, how can sulfur inhibit pollen tube growth? Moreover, does sulfur have the same effect on other species? The main objective of the present study is to clarify the mode of action of sulfur on the ultrastructure of the Nadorcott mandarin stigma and style. To fulfill this goal, untreated flowers and flowers treated with sulfur were pollinated 24 h later. The treated and untreated stigmas were analyzed and compared with several microscopy techniques. The main results showed that sulfur specifically caused an alteration to the outer layer of stigma papillary cells. This marked alteration resulted in papillary cells losing their functionality due to the deterioration and degradation of their cellular structure. Basal papillae, the stigmatic tissue and stylar canals also underwent major alteration. Sulfur also modified the quantity and uniformity distribution of the stigmatic exudate. All these alterations collectively prevented pollen tube development inside the stigma. These effects have been observed in several *Citrus* species and varieties, and in some other horticultural species, which suggests a generic (non species-specific) action.

Keywords: sulfur; pollen tube; seedless; *Citrus*; stigma; papillary cells; Nadorcott; exudate



Citation: García-Breijo, F.; Reig, J.; Cebrián, N.; Garmendia, A.; Beltrán, R.; Zornoza, C.; Merle, H. Ultrastructural Evidence Elucidates the Mode of Action of Sulfur in Preventing Pollen Tube Development in Stigma of *Citrus* cv. Nadorcott and Other Horticultural Species. *Agronomy* **2023**, *13*, 1643. <https://doi.org/10.3390/agronomy13061643>

Academic Editor: Concetta Licciardello

Received: 28 April 2023

Revised: 12 June 2023

Accepted: 16 June 2023

Published: 19 June 2023



Copyright: © 2023 by the authors. Licensee MDPI, Basel, Switzerland. This article is an open access article distributed under the terms and conditions of the Creative Commons Attribution (CC BY) license (<https://creativecommons.org/licenses/by/4.0/>).

1. Introduction

Successful sexual reproduction in angiosperms depends on a series of interactions between pollen grain and different gynoecium tissues. This process includes pollen grain germination on the stigma, pollen tube development and growth through the stigma and style and, ultimately, successful ovule fertilization [1–5]. These interactions likely involve complex communication, controlled by a genetic system that regulates the necessary biochemical and molecular environments: protein–protein or simple molecules, such as water, ions, lipids, sugars and calcium [3,4,6,7]. In angiosperms, a specialized set of tissues has evolved that interact with the pollen tube and facilitate its access to the female gametophyte [8–11]. Two of the most notable events are the specialization of a receptive surface on the stigma and transmitter tissue [10,12–14].

In many different species, pollen tubes begin to grow at the stigma-style interface before reaching the style [12,15,16]. In contrast, most eudicots and monocots show a syncarpic gynoeceum in which the pollen tube, after stigmatic germination, passes through the style to reach the locule of the ovary and ovule [16].

Angiosperm stigmas display considerable diversity in terms of both the receptive surface and the amount of secreted exudate present in the receptive stage [2,17–19]. In some families, a thin film covers the cuticle of stigma papillae [7,20–23]. This layer appears to be the site of the recognition reaction during pollination [2,17–19]. The pellicle that covers papillae is present only in the families with a “dry” stigma [24–26]. Many other families show a moist “wet” stigma that, in the receptive stage, is covered by a sticky secretion product [27–30]. In this exudate, both self- and cross-pollen germinate, and the recognition reaction occurs after penetrating stylar tissue (see de Nettancourt [31] for a review). *Citrus* species have a moist stigma with abundant exudate and a hollow style that contains numerous canals [32–34]. Histochemical and biochemical analyses of the stigmatic exudate show that it is heterogeneous, and is composed of lipids, polysaccharides and proteins. Cresti et al. [33] evaluated the stigma of *Citrus × limon* by scanning electron microscopy (SEM), and evaluations of fresh tissues showed that papillae are completely covered by a superficial exudate. The cv. Nadorcott flowers studied herein also have a “wet”-type stigma.

There is no evidence that pollen tubes obtain nutrients from the stigma exudates of species with wet stigmas [9,35–37], despite some speculation to the contrary [38]. Furthermore, in many species, the stigmatic tissues below the stigmatic surface anatomically and cytologically differ from the transmitting tissue in the style, and perform no secretory function [33,39,40].

In the style, the canal and transmitting tissue supply an extracellular secretion that is incorporated into the pollen tube to allow its heterotrophic growth [41,42], and which differs from pollen tube autotrophic growth on the dry stigma [42,43]. The transmitter tissue of the style is composed of highly active secretory cells that are characterized by the production of an extensive extracellular matrix (ECM) [44,45]. The actual roles played by this ECM are currently unknown, but proposed functions include the mechanical and chemotropic driving of the pollen tube [46–57] and pollen tube nutrition [48,58,59].

In relation to their transmission function and anatomy, styles can be classified into three different types: open, closed or semiclosed [7]. In *Citrus* sp., styles are open or semiclosed. In open styles, the ultrastructure of epithelial cells has been studied in some species, and is characterized by the presence of an abundant rough endoplasmic reticulum (RER), generally with cisterns in parallel to the external tangential wall, vacuoles, numerous mitochondria, well-developed plastids containing grana and lipid plastoglobules in numerous dictyosomes and vesicles [32,60–70].

Ciampolini et al. [32] found that the internal tangential walls of *Citrus × limon* (L.) Osbeck are formed by two layers: the original outer layer and the internal layer are formed by the subsequent deposition of abundant materials of different origins. In *Citrus × limon* [32] and *C. caroliniana* [69], significant activity in dictyosomes has been observed. Furthermore, the appearance of the stylar canal material is ultrastructurally heterogeneous, and is made up of polysaccharides, proteins and lipids that presumably provide nutrients for pollen tube growth [32].

Preventing the fertilization process can be useful for agronomic and plant breeding purposes. Seedless fruit, new crops through controlled crosses, triploid hybrids, etc., are some of the main objectives of agronomic research, which requires in-depth knowledge of the pollen-stigma interaction. For example, obtaining seedless mandarins has frequently been the objective of citrus farmers [71].

Recently, two studies have been published on using sulfur to avoid seeds being present in mandarins [72,73]. Elemental sulfur (S8) applied to Nadorcott stigmas inhibits pollen tube growth [72]. When this elemental sulfur is applied as an agronomic treatment to adult Nadorcott trees during the flowering period, it significantly reduces the seed number per

fruit compared to controls. In this study, six different products were tested in the field, but only sulfur showed good effectiveness, with 87% seed reduction [73]. However, what is the mode of action of sulfur? When applied to the stigma, how can sulfur inhibit pollen tube growth? Does it act on the pollen grain, or on the tissues of the gynoecium? Is it a cell division inhibitor? Does sulfur have the same effect on other species?

The main objective of the present study is to clarify the mode of action of sulfur on the ultrastructure of the Nadorcott mandarin stigma and style. Additionally, preliminary evidence is provided for its effect on other citrus varieties and other horticultural species. To fulfill this goal, flowers were either treated with sulfur or left untreated, then pollinated. The treated and untreated stigmas were analyzed and compared by epifluorescence microscopy (EFM), light microscopy (LM), transmission electron microscopy (TEM) and scanning electron microscopy (SEM).

2. Materials and Methods

2.1. Plant Material

Most observations (LM, SEM and TEM) were made on Nadorcott mandarin flowers. Nadorcott mandarin, also known as 'Afourer', is a hybrid of cv. Murcott (Murcott is a tangor hybrid of tangerine and orange, *Citrus reticulata* Blanco × *C. sinensis* (L.) Osbeck) and an unknown pollinator parent [74]. For this variety, treatments were performed on the flowers of the adult cv. Nadorcott trees growing in a commercial orchard in the municipal district of Montserrat (Valencia Province, Spain) (39°21'35" N 0°32'44" W; altitude 150 m) during the flowering period of April 2017 and 2018. Orchard management was carried out under standard cultural conditions with no other treatments during the flowering period, except for the experimental treatments.

From the *Citrus* genus, the treated and untreated flowers of cv. Clemenules (*Citrus clementina* Hort. ex Tan), cv. Fina (*Citrus clementina* (Hort. ex Tan), cv. Murcott (*Citrus reticulata* Blanco), cv. Nova (*C. clementina* × [*C. paradisi* × *C. tangerina*]), cv. Arrufatina (*Citrus clementina* Hort. ex Tan) and Verna lemon (*Citrus* × *limon* (L.) Burm.f.) were observed by epifluorescence UV. Preliminary observations were also made on cucumber (*Cucumis sativus* L.), eggplant (*Solanum melongena* L.) and watermelon (*Citrullus lanatus* (Thunb.) Matsumara & Nakai). In all these cases, to obtain the treated and untreated flowers, plants were grown in a phytotron chamber under controlled spring conditions (day 13 h, 22 °C, night 11 h, 12 °C) in 2018.

2.2. Treatments

Three adult cv. Nadorcott trees were randomly selected from the orchard to use flowers for treatments. Immediately before the flowering period, the three trees were covered with nets to avoid unwanted pollination. Upon anthesis, flowers were treated and pollinated 24 h later. Two treatments were included in the experiment: (1) the positive control (C+), where stigmas were gently rubbed with a clean brush with no product; and (2) the sulfur treatment (S), where stigmas were gently rubbed with a brush with elemental sulfur (S8). Approximately 0.5 g of sulfur was applied to each stigma. For pollinations (24 h after treatment), the flowers of a compatible variety (cv. Nova) growing close to the experimental plot (<than 150 m) were collected on the same day. The donor pollen were brushed gently against cv. Nadorcott stigmas.

For the species growing in the phytotron chamber (other *Citrus* varieties and horticultural species), treatments were performed in the same way as for cv. Nadorcott: upon anthesis, flowers were treated with sulfur (S) or were left untreated (C+) and were forced-pollinated with compatible pollens 24 h later.

2.3. Analyzed Tissues

The Nadorcott stigma can be divided into two zones (Figure 1): a superficial glandular or stigmatic zone (StZ) formed by papillae; and a deeper non glandular region or stigmatoid

tissue (StT) (Figure 1b) formed by parenchymal cells, which is in continuity with that surrounding styler canals (SC) (Figure 1a,b).

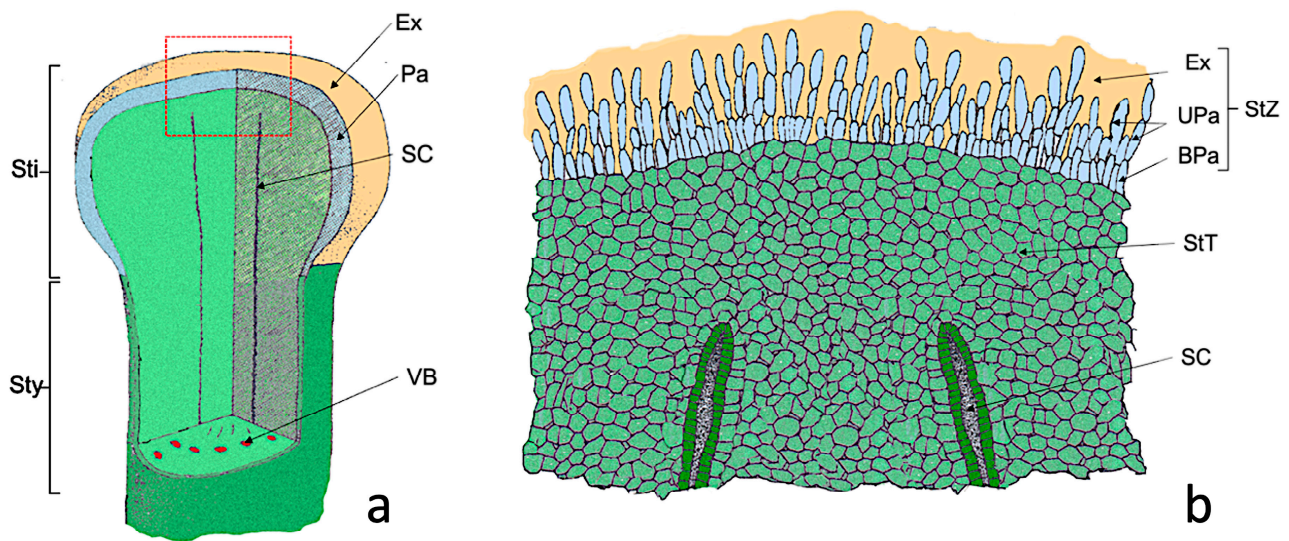


Figure 1. Scheme of the Nadorcott stigma. (a) Diagram showing the part of the stigma (Sti) and the upper style part (Sty). (b) Detail of the red box shown in (a), where the cellular organization of the stigma is observed. Abbreviations: BPa, basal papillae; Ex, exudate; Pa, papillae; SC, styler canal; StT, stigmatoid tissue; StZ, stigmatic zone; UPa, upper papillae, VB, vascular bundle. Modified from Cresti et al., 1982 [33].

In the stigmatic glandular area (stigmatic zone, StZ), two regions can be distinguished: one made up of elongated papillary cells (UPa, upper papillae) and a second of more rounded basal papillary cells (BPa, basal papillae) (Figure 1b). After anthesis, papillae were completely covered by the exudate (Ex). Therefore, the differences between the treated (S) and untreated (C+) flowers were referred to as: (1) elongated papillary cells region; (2) basal papillary cell region; (3) stigmatoid tissue; (4) styler canals; (5) exudate.

2.4. Flower Sampling

Flowers were collected 5 days after pollination. For Nadorcott, at least 10 flowers per treatment and tree ($\times 3$) were sampled early in the morning. For the other species, at least five flowers per treatment and plant ($\times 3$ per species) were also sampled early in the morning. Anthers and perianths were removed, and pistils were immediately fixed in: (a) a Formalin-Aceto-Alcohol (FAA) solution (10 mL of 37% formaldehyde, 50 mL of 95% ethyl alcohol, 5 mL of glacial acetic acid, 35 mL of distilled water) to work under LM, epifluorescence microscopy (EFM) and SEM conditions, and were subsequently stored at 4 °C in the refrigerator until analyzed; or (b) with modified Karnovsky (2% paraformaldehyde and 2.5% glutaraldehyde [75]) to work under TEM conditions. The samples for TEM were fixed and dehydrated as described in Molins et al. 2018 [76].

2.5. Observation by Epifluorescence Microscopy, (EFM)

For the autofluorescence-stained sections, flowers were sectioned longitudinally on ca. 20 μm with a freezing microtome (Leica CM 1325; Leica Microsystems Nussloch GmbH, Nußloch, Germany). Sections were stained with aniline blue fluorochrome (0.1% in PBS buffer) for 15 min, subsequently washed with distilled water and mounted on microscope slides to be observed by EFM. Sections were examined by EFM to analyze stigmas and style. All the LM and EFM observations were made by an Olympus Provis AX 70 fluorescence microscope (Olympus Optical Co., Ltd., Hamburg, Germany) equipped with an Infinity 2–3 C Lumenera® (Lumenera Corp., Ottawa, ON, Canada) digital camera and analyzed by the “Infinity Analyze” software, v.6.4.1. For fluorescence microscopy, an Olympus U-ULS

100 HG epifluorescence system with a U-MWBV cube (excitation filter 400–440 nm, dichroic mirror 455 nm, barrier filter 475 nm) was used.

2.6. Observation by Light Microscopy (LM)

The samples fixed with FAA were embedded in Spurr's resin following the manufacturer's instructions. Semithin sectioning (1.5 μm) was performed by a Sorvall MT 5000 Ultra Microtome (Girard-Dupont, Detroit, MI, USA) with glass blades (45°) obtained from a special glass (Glass Strips 6.4 mm from Leica) in a knifemaker (Reichert-Jung, Wien, Austria). These samples were dyed with toluidine blue [77] at 1%. To observe preparations, an Olympus Provis AX-70 light field microscope was used, and pictures were taken with an Infinity 2CCD color digital camera (Lumenera Corp., Ottawa, ON, Canada), and were processed with the image acquisition software 'Infinity Analyze[®] 7' v. 7.1.0 (Lumenera Corp.) and then later by the Photoshop program CC[®] 2018.

2.7. Observation by Transmission Electron Microscopy, (TEM)

The Karnovsky-fixed and post-OsO₄-fixed samples were dehydrated in ethanol series (50%, 70%, 80%, 96% and absolute) for 2 \times 15 min each. Samples were embedded in Spurr's resin following the manufacturer's instructions. Ultrathin sections (80 nm) were cut, and were mounted and stained with 10% uranyl acetate and 0.1% lead citrate using the 'Synaptek Grid-Stick Kit' following the manufacturer's instructions. The ultrathin sections were observed by a JEOL JEM-1010 (100 kV) electron microscope (Jeol Deben Amt, Suffolk, UK), equipped with a MegaView III digital camera and the 'AnalySIS' image acquisition software (Olympus, Tokyo, Japan) (Electron Microscopy Service of the Polytechnic University of Valencia).

2.8. Observation by Scanning Electron Microscopy, (SEM)

Several FAA-fixed samples were used for the SEM observations. Samples were dried in a critical point dryer (Leica Cpd300; Leica Microsystems Nussloch GmbH, Nußloch, Germany). Later, gold sputtering was carried out. Samples were observed by Field Emission SEM (FESEM Ultra 55, Zeiss Oxford Instruments of the Electron Microscopy Service of the Polytechnic University of Valencia) with a SE2 Secondary Electron Detector. Work was performed in the low vacuum mode (70 Pa) at an accelerating voltage of 2 kV.

3. Results

3.1. Pollen Tube Development Inside the Nadorcott Stigma

The longitudinal autofluorescence-stained freeze sections showed numerous pollen grains and pollen tubes developing inside the stigma of the untreated flowers (C+; Figure 2a). The number of pollen grains attached to the stigma was much smaller and no pollen tube development was observed in the flowers treated with sulfur and pollinated 24 h later (sulfur treatment, S; Figure 2b). This result was observed in all the treated (S) and untreated (C+) Nadorcott mandarin flowers. Pollen tubes were observed as fluorescent threads inside the stigma (Figure 2a, PT). In both cases (C+ and S), the pollen grains on the stigma surface, papillary cells and style canals were noted (Figure 2a,b, PG, Pa and SC).

3.2. General View of the Untreated and Treated Nadorcott Stigmas

The semithin longitudinal sections of the control flowers (C+) showed intact papillary cells (Figure 3a–f), while the same sections of the sulfur-treated flowers (Figure 4) revealed a marked alteration to the glandular zone (papillary cells). In more detailed sections, this alteration mainly affected the upper papillary cells and the exudate (Figure 4c–e), and affected basal papillary cells and stigmatoid tissue to a lesser extent. However, stylar canals were also quite affected.

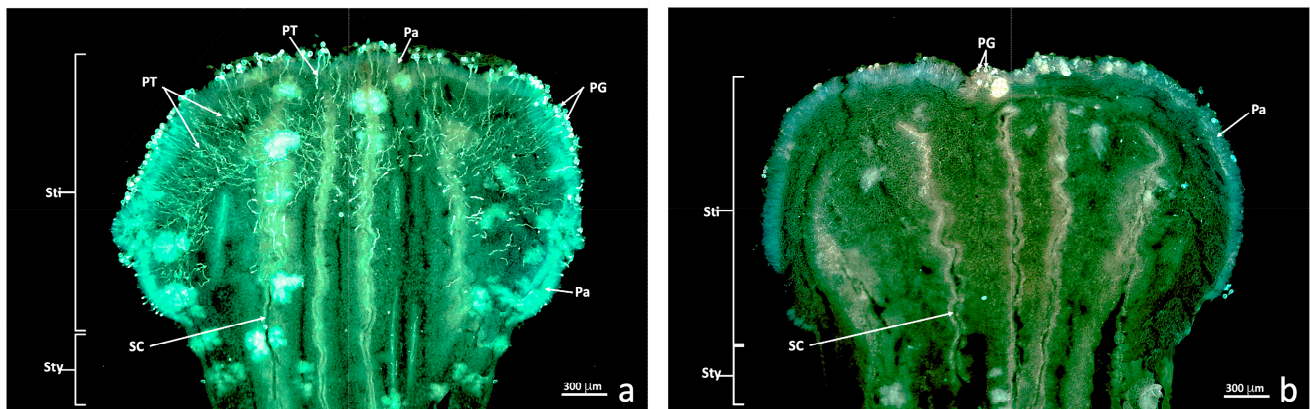


Figure 2. Epifluorescence UV sections of the untreated and treated stigma. Longitudinal freeze-cut sections stained with aniline blue and viewed under epifluorescence UV. (a) Untreated stigma (C+); (b) Stigma treated with sulfur (S). Abbreviations: Pa, papillae; PG, pollen grain; PT, pollen tube; SC, stylar canal; Sti, stigma; Sty, style.

Occasionally in the same flowers treated with sulfur, affected areas were observed where papillae appeared to be considerably altered, but also unaffected areas with entire papillae (Figure 4b). This distribution of altered and unaltered areas indicated that applying sulfur to this flower was probably not uniform all over the stigma surface. In these cases, some of the pollen grains that fell in these unaltered areas germinated and produced barely developed pollen tubes along the style. The thickness of the stigmatic glandular area (StZ) was about $125 \pm 30 \mu\text{m}$. Both LM and TEM revealed that the stigmatic zone was not structurally homogeneous, with an area of elongated papillary cells and an area with basal papillary cells (Figures 3 and 4).

3.3. Region of Elongated Cells (Upper Papillae)

In the untreated flowers, the upper papillary cells possessed many dictyosomes, amyloplasts, mitochondria and an RER (Figure 5). Nuclei were located centrally or basally. They presented some medium-sized vacuoles. The RER (Figure 5e,f,i,j) and dictyosomes (Figure 5g,j) were very active and produced many secretion vesicles. Many of these vesicles were close to or in contact with the plasma membrane (Figure 5f,h). Some lipid bodies were also observed, and some vacuoles containing lipid material developed (Figure 5) that secreted and accumulated near the cell wall (Figure 5g,h). The granular material that appeared in the exudate was similar in structure and electron density terms to the content of Golgi vesicles. These cells performed considerable secretory activity. Cell contact was extensive and uniform.

In the flowers treated with sulfur, a marked structural alteration to stigmatic papillae took place, especially the upper ones (Figure 6). Many of the upper papillae collapsed because their cell walls softened and due to internal protoplast disorganization. Loss of cellular turgor occurred because of hypotonic processes, which led to large spaces appearing between the cell wall and the cell membrane (Figure 6). Consequently, many plasmodesmata disappeared. In addition, amyloplasts, which abounded in the papillae of the untreated stigmas, completely disappeared in the affected ones. The presence of RER tubules, dictyosomes and polyribosomes was barely noted in these affected cells (Figure 6e). The number of secretion vesicles from dictyosomes lowered and it is usual for marked degradation of cellular content to take place (Figure 6).

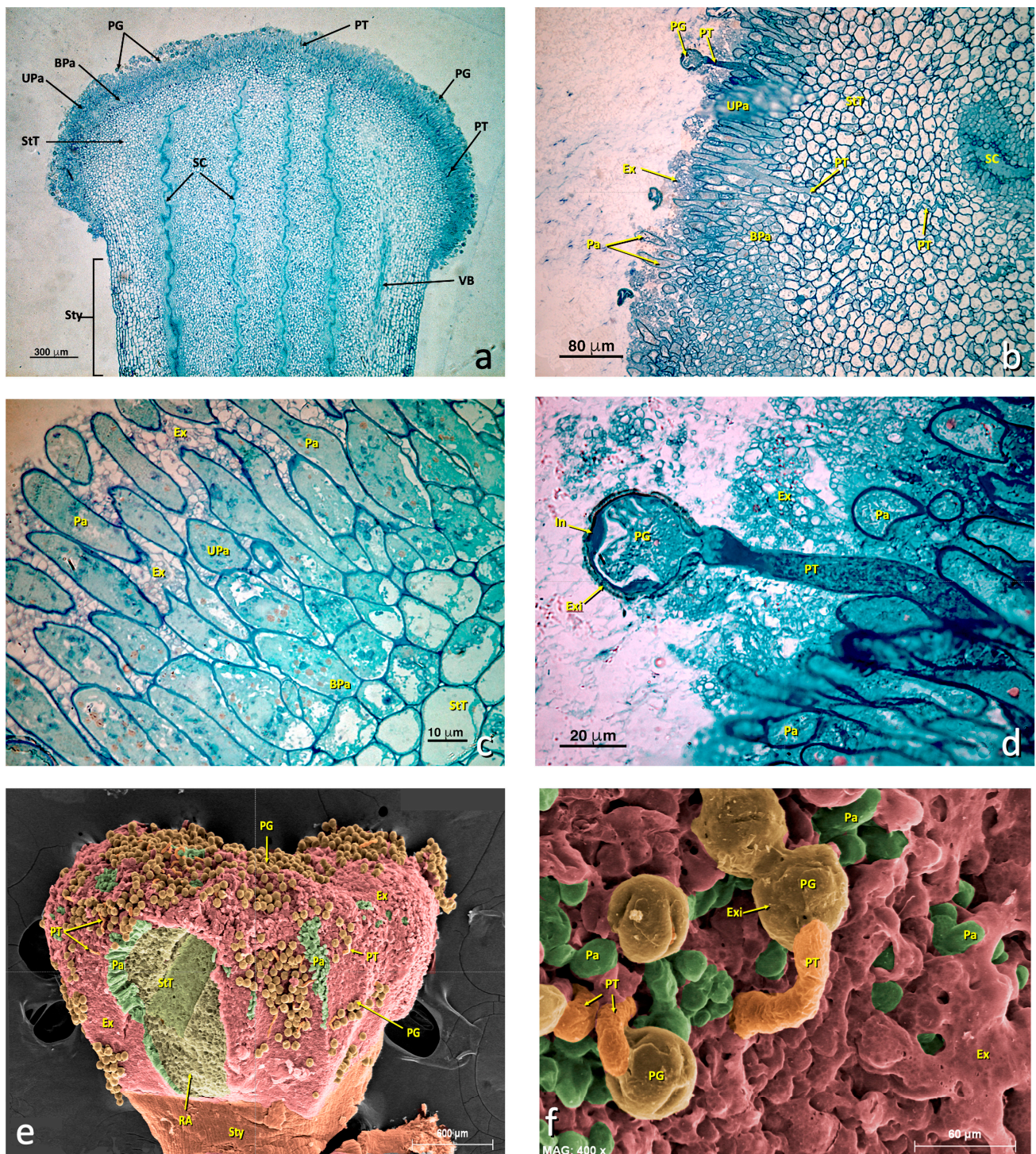


Figure 3. General views of an untreated stigma. (a–d) Light micrographs of the longitudinal sections of the semithin sections stained with toluidine blue. (e–f) SEM micrographs with a false color. (a) General stigma view. (b) Detail of an area of the glandular layer (papillae) showing some pollen grains producing a pollen tube. (c) Detail of the glandular area. (d) Detail of a germinating pollen grain. (e) General stigma view (SEM). (f) Detail of a germinating pollen grain (SEM). (a) bar 300 μm ; (b) bar: 80 μm ; (c) bar: 10 μm ; (d) bar: 20 μm ; (e) bar: 600 μm ; (f) bar: 60 μm . Abbreviations: BPa, basal papillae; Ex, exudate; Exi, exine; In, intine; Pa, papillae; PG, pollen grain; PT, pollen tube; RA, ripped area; SC, stylar canal; StT, stigmatoid tissue; Sty, style; StZ, stigmatic zone; Upa, upper papillae; VB, vascular bundle.

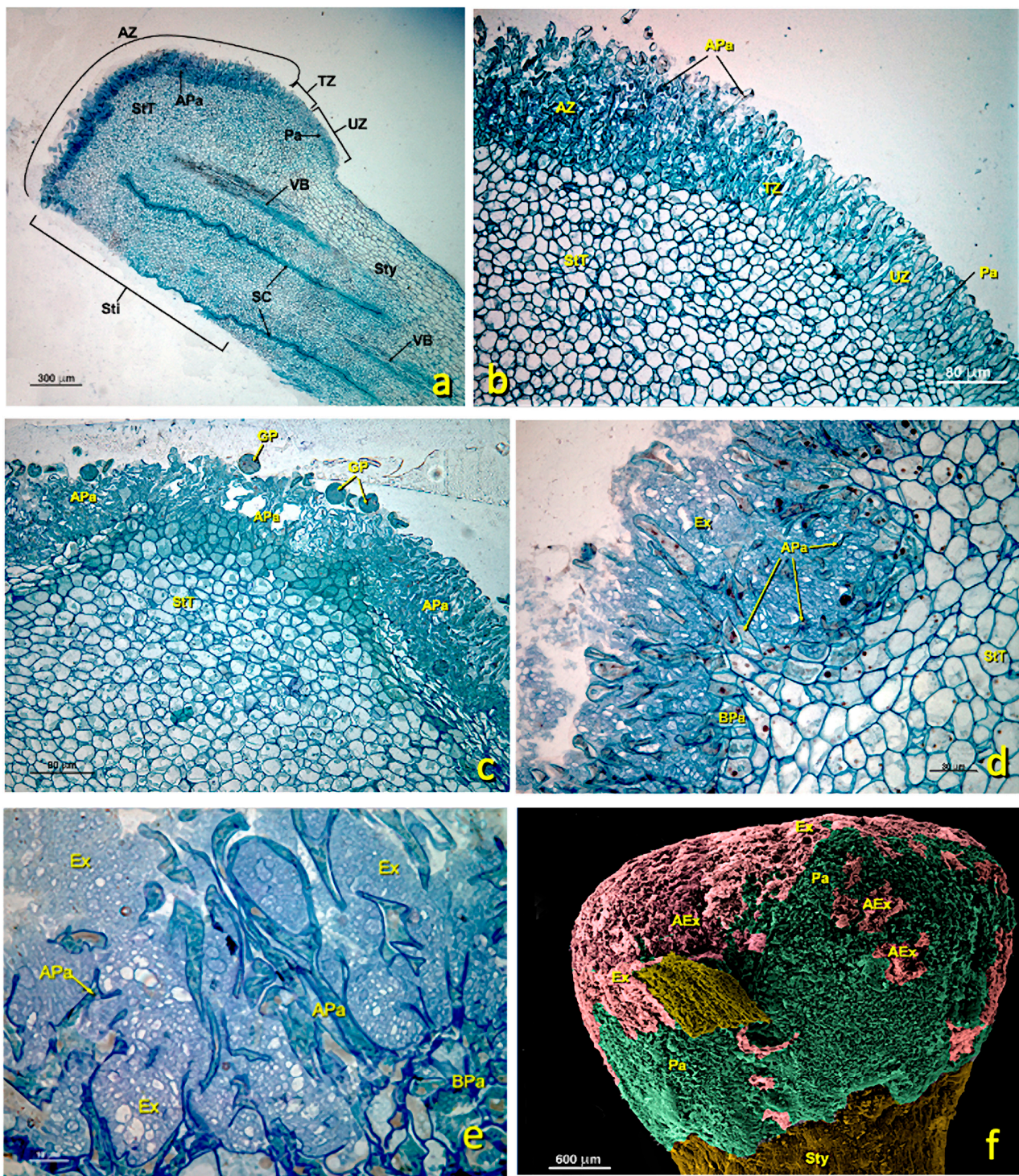


Figure 4. General views of a treated stigma. (a–f) Longitudinal semithin sections stained with toluidine blue. (a) General stigma view showing the areas affected and not affected by treatment. (b) Detail of the transition zone between an affected zone and another unaffected zone. (c–e) Details of affected areas showing the appearance of papillae of the glandular stigma area. (f) General stigma view (SEM). (a) bar 300 μm ; (b) bar: 80 μm ; (c) bar: 80 μm ; (d) bar: 30 μm ; (e) bar: 10 μm ; (f) bar: 600 μm . Abbreviations: AEx, altered exudate; APa, affected papillae; AZ, affected zone; BPa, basal papillae; Ex, exudate; Pa, papillae; PG, pollen grain; SC, style channel; Sti, stigma; Sty, style; StT, stigmatoid tissue; TZ, transition zone; UZ, unaffected zone; VB, vascular bundle.

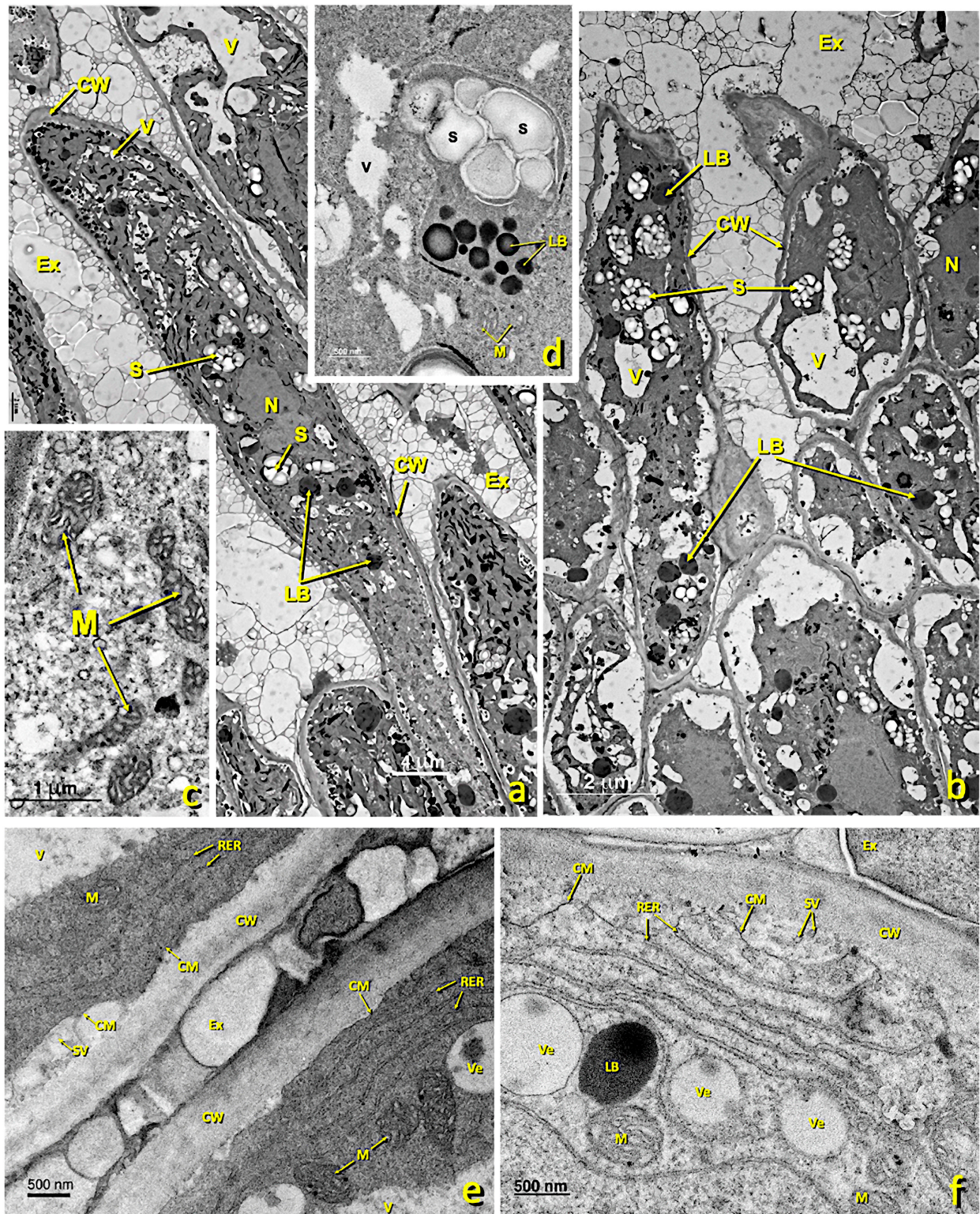


Figure 5. Cont.

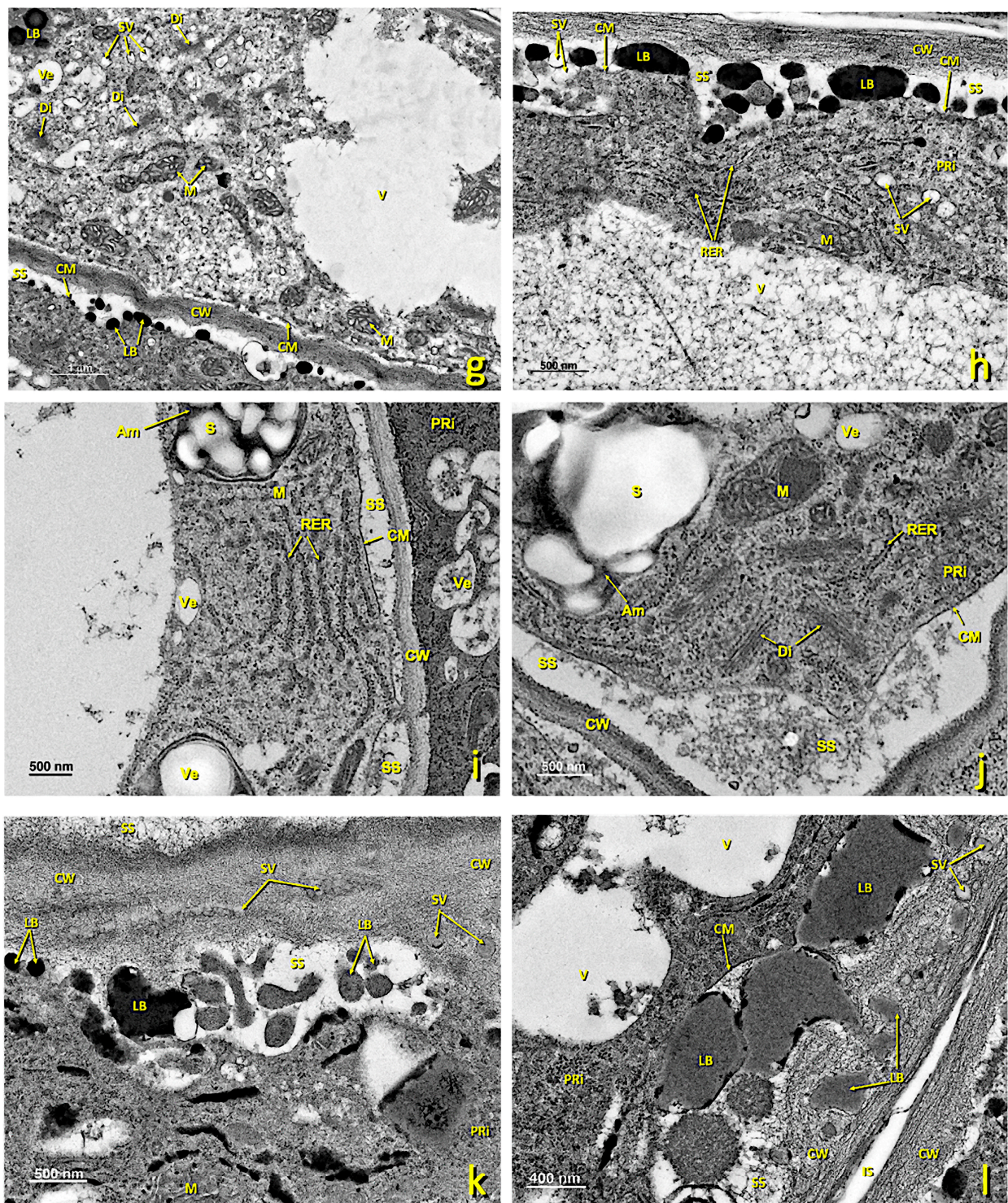


Figure 5. Upper papillae of an untreated stigma. Transmission electron (TEM) micrographs of the upper papillae present in the glandular area of an untreated stigma. (a,b) General papillae view. (c) Detail of a zone rich in mitochondria. (d) Detail of a zone rich in starch (amyloplast) and lipid droplets. (e) Detail of an area close to the cell wall rich in the rough endoplasmic reticulum. (f) Detail of a zone rich in the rough endoplasmic reticulum and secretion vesicles. (g) Detail of a zone rich in mitochondria, dictyosomes and lipid bodies. (h–j) Details of cytoplasmic areas close to the cell wall rich in dictyosomes, the rough endoplasmic reticulum and secretion vesicles. (k,l) Detail of areas close to the cell wall where numerous secretory vesicles and lipid bodies and droplets can be seen in the secretion space and inside the cell wall. (a) bar: 4 μm ; (b) bar: 2 μm ; (c) bar: 1 μm ; (d) bar: 500 nm; (e) bar: 500 nm; (f) bar: 500 nm; (g) bar: 500 nm; (h) bar: 500 nm; (i) bar: 500 nm; (j) bar: 500 nm; (k) bar: 500 nm; (l) bar: 400 nm.

(e) bar: 500 nm; (f) bar: 500 nm. (g) bar: 1 μ m; (h) bar: 500 nm; (i) bar: 1 nm; (j) bar: 500 nm; (k) bar: 500 nm; (l) bar: 400 nm. Abbreviations: Ex, exudate; CM, cell membrane; CW, cell wall; LB, lipid bodies; M, mitochondria; N, nucleus; RER, rough endoplasmic reticulum; S, starch; SV, secretion vesicle; V, vacuole; Ve, vesicle. Am, amyloplast; Ex, exudate; CM, cell membrane; CW, cell wall; Di, dictyosomes; IS, intercellular space; LB, lipid bodies; M, mitochondria; N, nucleus; PRi, polyribosomes; RER, rough endoplasmic reticulum; S, starch; SS, secretion space; SV, secretion vesicle; V, vacuole; Ve, vesicle.

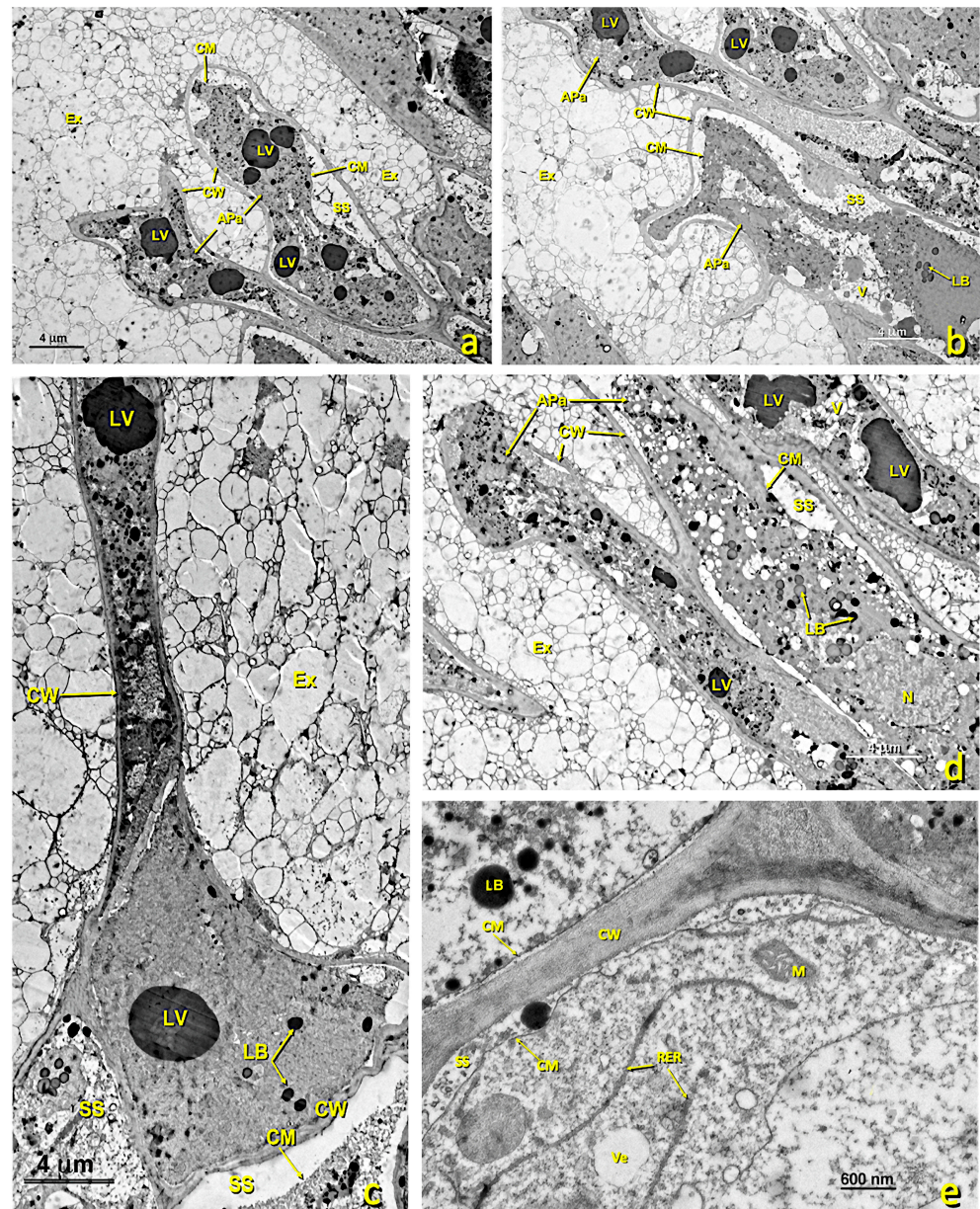


Figure 6. Upper papillae of a treated stigma. Transmission electron micrographs (TEM) of the affected papillae present in the glandular area of the stigma. (a–d) General view of the different affected papillae in the upper part of the treated glandular area displaying the cellular collapse and the internal degradation undergone by these papillae. (e) Detail of an area near the wall, where a few RER tubules and secretion vesicles can be seen. (a) bar: 4 μ m; (b) bar: 4 μ m; (c) bar: 4 μ m; (d) bar: 4 μ m; (e) bar: 600 nm. Abbreviations: APa, affected papillae; CM, cellular membrane; CW, cellular wall; Ex, exudate; LB, lipid bodies; LV, lipid vesicles; N, nucleus; M, mitochondrion, RER, rough endoplasmic reticulum; SS, secretion space; V, vacuole; Ve, vesicle.

3.4. Basal Papillary Cell Region

In the untreated flowers, this region consisted of 2–3 layers of secreting cells with walls similar to those of elongated papillae. Intercellular spaces hardly appeared (Figure 7a). In mature cells, large vacuoles and numerous amyloplasts were noted (Figure 7a,d), as were flattened tubules of the RER (Figure 7c) and numerous mitochondria (Figure 7c). In the areas of the membrane close to cell walls and in contact with the areas of exudate or intercellular spaces, numerous vesicles and lipid bodies were seen in the secretion space (Figure 7e), which later accumulated in the cell wall, where they merged (Figure 7f). From this region, these lipid bodies penetrated the intercellular spaces between the pointed papillary cells, and eventually covered the stigma. In this stage, plastids were very starchy, had dense stroma and were surrounded by RER cisternae.

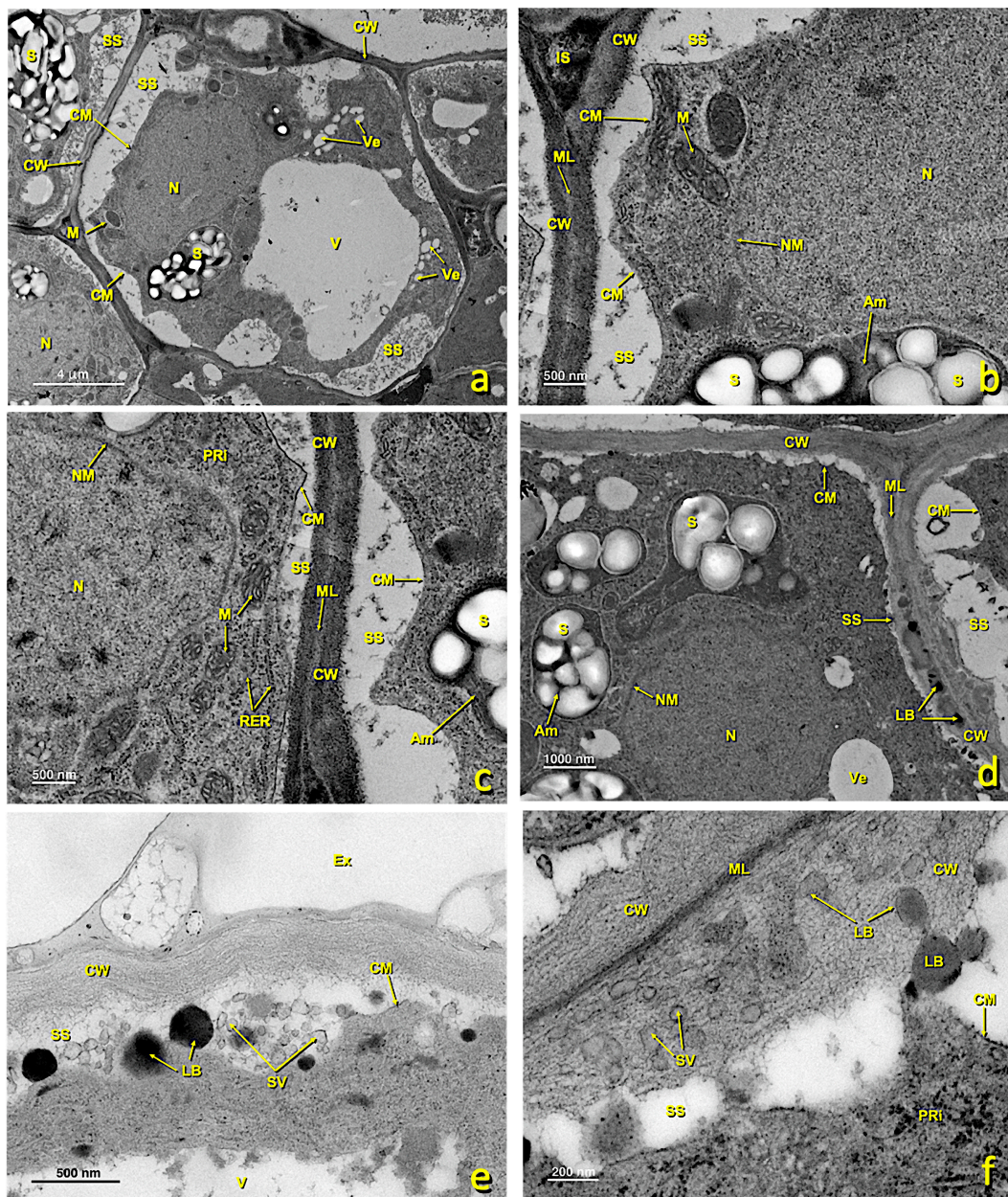


Figure 7. Basal papillae of an untreated stigma. Transmission electron (TEM) micrographs of the basal papillae present in the glandular area of an untreated stigma. (a) General basal papillae cell view. (b,c) Details of areas showing part of the nucleus and several mitochondria. (d) Zone showing the nucleus and numerous amyloplasts. (e) Area of the cytoplasm close to the wall with numerous secretion. (f) Area of the cytoplasm close to the wall with numerous secretion.

secretion vesicles and lipid bodies. (f) Area of the wall where numerous secretion vesicles and lipid bodies can be seen between its fibers. (a) bar: 4 μm ; (b) bar: 500 nm; (c) bar: 500 nm; (d) bar: 1000 nm; (e) bar: 500 nm; (f) bar: 200 nm. Abbreviations: Am, amyloplast; Ex, exudate; CM, cell membrane; CW, cell wall; Di, dictyosomes; IS, intercellular space; LB, lipid bodies; M, mitochondria; ML, middle lamella; N, nucleus; NM, nuclear membrane; PRi, polyribosomes; RER, rough endoplasmic reticulum; S, starch; SS, secretion space; SV, secretion vesicle; V, vacuole; Ve, vesicle.

In the treated flowers, basal papillae were also affected, albeit to a lesser extent than the upper ones. In some cells, the protoplast collapsed and the cellular structure was disorganized (Figure 8). As a consequence of collapse, large spaces appeared between membranes and the cell walls filled with granular content (Figure 8b,d,g). Organelles were considerably altered. RER cisterns were disorganized and scattered throughout the cytoplasm (Figure 8c,h). The vesicles of the low-density content abounded, but hardly any starch remained in the plastids. Mitochondria were still visible, but were fewer than in the untreated papillae.

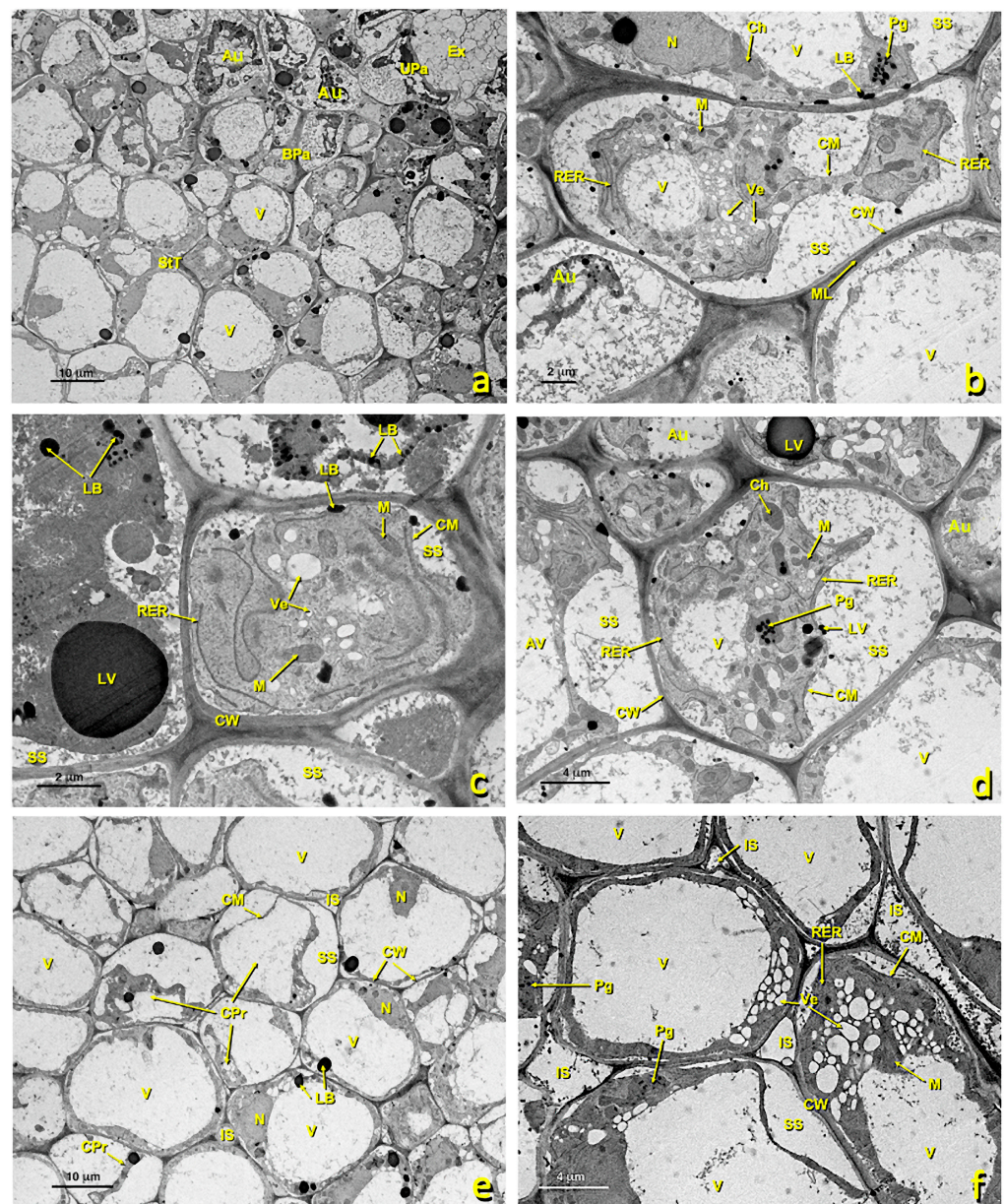


Figure 8. Cont.

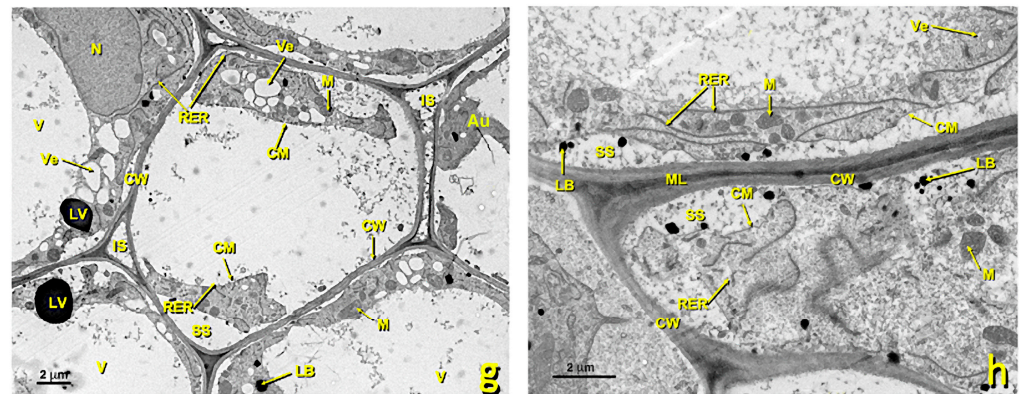


Figure 8. Basal papillae and stigmatoid tissue of a treated stigma. Transmission electron (TEM) micrographs of the basal papillae (a–d) and of the stigmatoid tissue (e–h) of a treated stigma. (a) bar 10 µm; (b) bar: 2 µm; (c) bar: 2 µm; (d) bar: 4 µm; (e) bar: 10 µm; (f) bar: 4 µm; (g) bar: 2 µm; (h) bar: 2 µm. Abbreviations: Au, autophagosome; BPa, basal papillae; Ex, exudate; Ch, chloroplast; CM, cell membrane; CPr, collapsed protoplast; CW, cell wall; IS, intercellular space; LB, lipid bodies; LV, lipid vesicle; M, mitochondria; ML, middle lamella; N, nucleus; Pg, plastoglobuli; RER, rough endoplasmic reticulum; SS, secretion space; StT, stigmatoid tissue; UPa, upper papillae; V, vacuole; Ve, vesicle.

3.5. Stigmatoid Tissue

This tissue is made up of several layers of parenchymal cells that were, in the upper part, in contact with the glandular region and, in the deepest part, in continuity with the style. In the untreated flowers, parenchymal cells were generally rounded in cross-sections, highly vacuolated and rich in amyloplasts (Figures 3b and 9a). According to TEM, the main features of these cells included the presence of a large central vacuole and many amyloplasts containing large starch grains (Figure 9a). The presence of an abundant RER (Figure 9b), and many dictyosomes, polyribosomes (Figure 9d) and secretion vesicles (Figure 9b,c,e) was observed in these cells. This RER was close to the cell membrane, which would confirm the aforementioned exchange because plant cells lacked an internal environment and passed different nutrients through the plasmodesmata. In the mature stage, large intercellular spaces were present (Figure 9a and Figure S1c,d) through which pollen tubes grew before entering styler canals (Figure S1). Stigmatic tissue was continuous with the style.

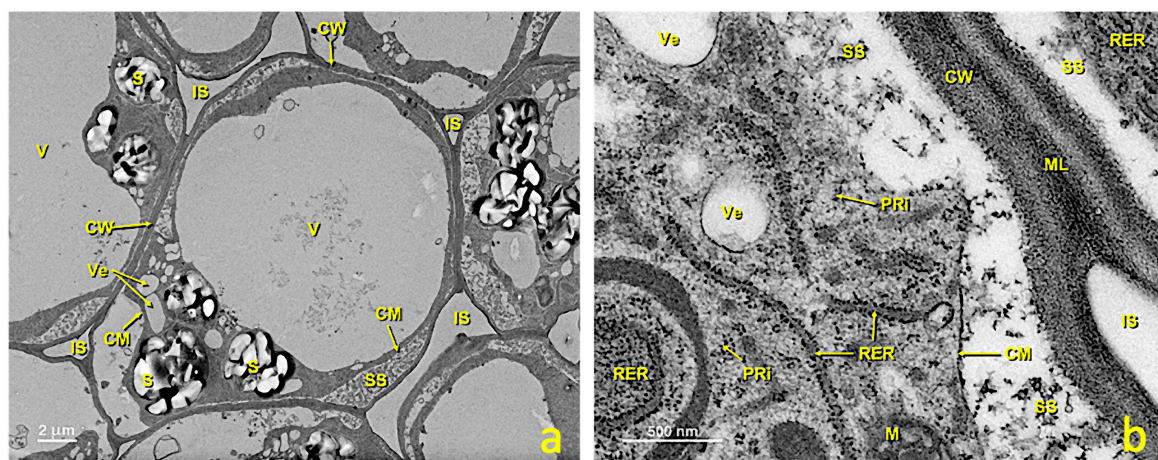


Figure 9. Cont.

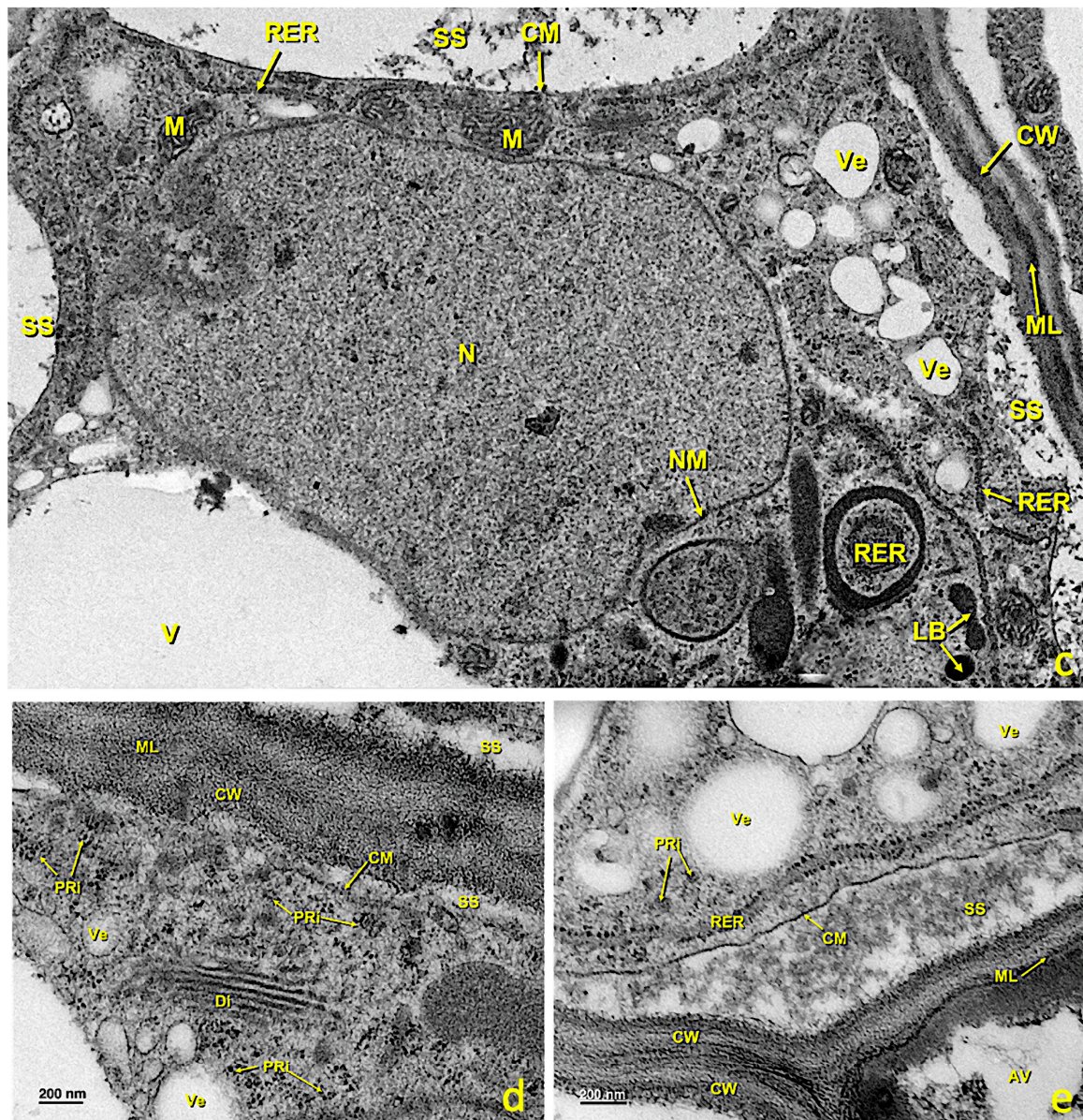


Figure 9. Stigmatic zone of an untreated stigma. Transmission electron micrographs (TEM) of the cells in the stigmatic zone. (a) General cell view. (b) Detail of an area close to the cell wall showing the rough endoplasmic reticulum tubules, polyribosomes and the secretion space. (c) Detail showing the nucleus and one part of the cytoplasm with an abundance of organelles related to the secretion of protein and polysaccharide material. (d) Detail of an area near the wall where numerous polyribosomes and a dictyosome can be seen. (e) Detail of an area near the wall where polyribosomes, secretion vesicles and the secretion space can be seen. (a) bar: 2 μm ; (b) bar: 500 nm; (c) bar: 500 nm; (d) bar: 200 nm; (e) bar: 200 nm. Abbreviations: Au, autophagosome; CM, cellular membrane; CW, cellular wall; Di, dictyosome; IS, intercellular space; LB, lipid bodies; N, nucleus; M, mitochondria; S, starch; ML, middle lamella; NM, nuclear membrane; PRi, polyribosome; RER, rough endoplasmic reticulum; SS, secretion space; V, vacuole; Ve, vesicle.

In the sulfur-treated flowers, the transition zone toward stigmatic tissue and the cells of this zone also underwent alterations. Many of them showed a collapsing protoplast, which made it very small (Figure 8e–h). Numerous vesicles appeared in the cytoplasm, and organelles became altered and disorganized. RER tubules were scattered, and the cytoplasm was highly degraded (Figure 8h). In many cases, intercellular spaces were filled with granular content (Figure 8f,g).

3.6. Styler Canals

In the middle of stigmatic tissue, near the glandular area, styler canals formed by cells of the canal and the styler duct appeared (Figure 3a,b and Figure 10). In the untreated flowers, canal cells were very rich in cytoplasm and their inner tangential wall was very thick (Figure 10d,e). The nucleus, which generally occupied the middle of the cell, was irregular in shape and contained only one nucleolus (Figure 10b,c). Numerous cytoplasmic organelles were seen. Dictyosomes, the endoplasmic reticulum (ER) and polyribosomes appeared mainly in the area of the cytoplasm close to the styler duct (Figure 10d), while mitochondria were distributed among them. Dictyosomes were very active, numerous and made up of several cisternae that produced many vesicles. These vesicles were observed free in the cytoplasm and close to or in direct contact with the plasma membrane (Figure 10e). The ER was of the rough type (RER); many stacked cisternae were arranged near the plasma membrane and mixed with dictyosomes. Ribosomes and polyribosomes were randomly distributed throughout the cell. Many mitochondria appeared and were elliptical in shape (Figure 10d,e). In the cytoplasm, particularly in the portion between the nucleus and the outer tangential wall, many autophagosomes were present. The most notable feature of these cells was the thickening of the inner tangential wall lining the canal (Figure 10d,e). Upon maturity, the walls, especially the wall in contact with the canal (inner tangential wall; 365.5 ± 32.6 nm), were much thicker than the outer tangential (100.2 ± 13.1 nm) and radial walls (179.1 ± 12.7 nm) (Figure 10a).

The internal tangential walls were covered by a very thin, continuous and apparently resistant film. This film adhered to the lateral walls, but was separated from the tangential wall by secreted material. The wall itself consisted of two layers (Figure 10e); the outer layer in contact with the styler canal was loose, granular and homogeneous; on the contrary, the inner layer is more electron-dense, fibrillar and homogeneous, and was at least twice as thick as the outer shell. Styler canals started very close to the glandular zone in stigmatic tissue and reached the locules of the ovary. Their lumen was 6 ± 2 μ m. Pollen tubes crossed stigmatic papillae, grew intercellularly between parenchymas, and then between canal cells (Figure S1c,d) toward the ovary. Upon maturity, the canal ducts filled with material were secreted by canal cells. This material was not continuous, because the portion provided by each cell remained enclosed by a fine persistent cuticle that originally covered the cell wall (Figure 10b,c). Most of the material was amorphous, low electron dense and granular. In addition, large aggregates of compact and clearly osmiophilic material (electron-dense) were present (Figure 10a,b). In addition, small masses of yet another material were observed, which was also homogeneous and compact, but less opaque to electrons (Figure 10a,b).

In the treated flowers, styler canals were also quite affected. The cells lining styler ducts (Figure 11) were considerably altered. They lost their shape due to the collapsing protoplast, and the structure seen in the untreated canals was lost. Marked cellular content disorganization occurred, with significant loss of cell organelles (mitochondria, RER, dictyosomes, etc.). The area where the granular material accumulated almost collapsed.

3.7. Effect on Exudate

In the receptive stage of an untreated flower (from anthesis), the stigmatic exudate almost completely covered the numerous papillae. This exudate was produced by papillae once they were in their mature state. The exudate allowed the union of pollen (Figure 3e) and its germination (Figure 3d,f). Subsequently, the pollen tube passed through the stigmatic tissue and reached styler canals (Figure S1c,d). The stigma of an untreated flower showed uniform exudate distribution (Figure 3e). Adhesion and germination of pollen grains were also observed (Figure 3f).

The flowers treated with sulfur showed a different aspect from the exudate (Figure 4e,f). In this case, the treated stigma displayed uneven exudate distribution and areas with altered exudate. The areas without exudate, the areas with altered exudate and those in which degraded materials were present were clearly observed in the treated stigma (Figure 4e,f,h).

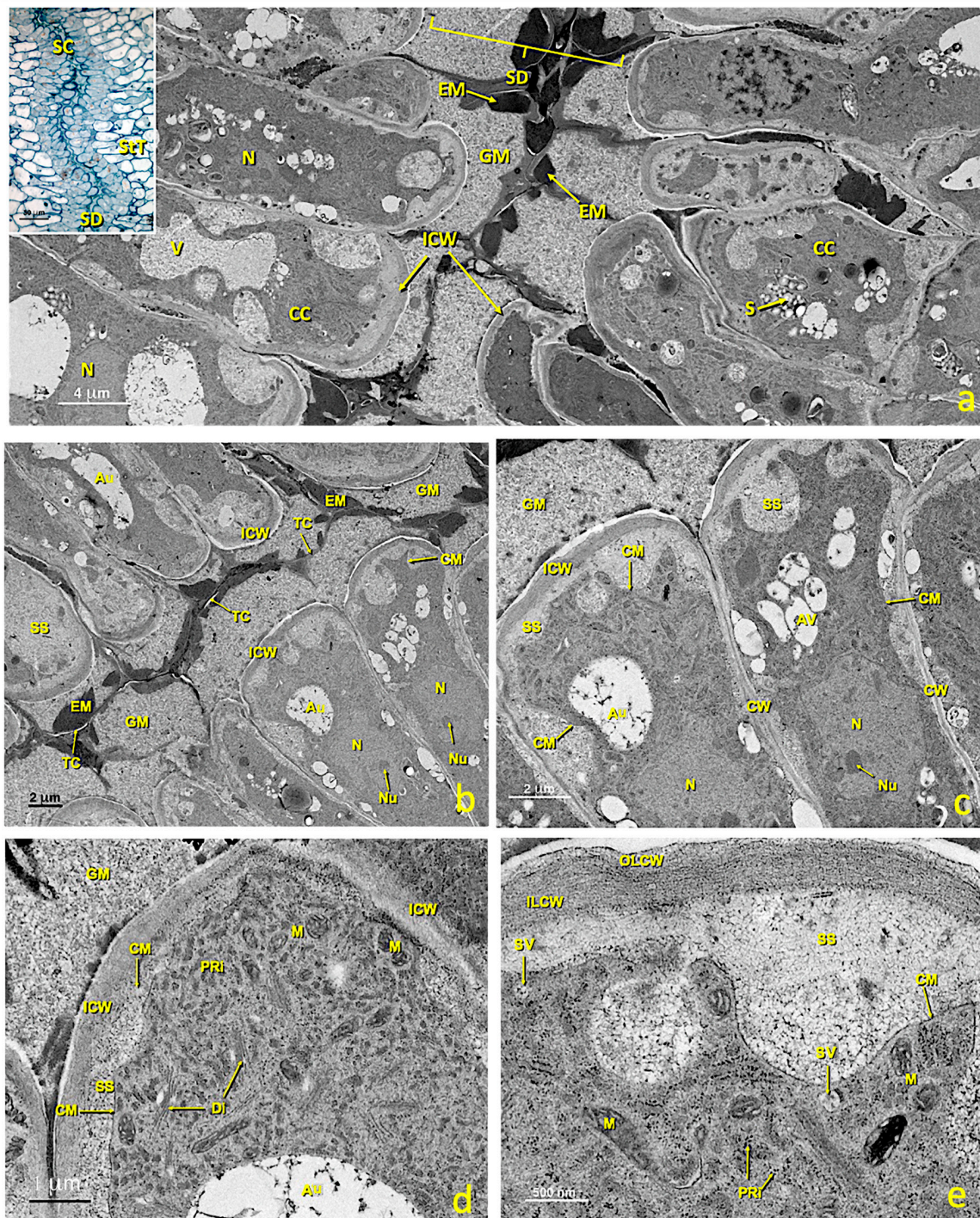


Figure 10. Stylar canal from flowers with an untreated stigma. Transmission electron micrographs (TEM) of a section of mature stylar canal cells. (a) View of the cells that form the stylar canal and the stylar duct. (b) Stylar duct detail. (c) Cross-section of mature canal cells with considerably thickened inner tangential walls. (d) Detail of a canal cell showing its thickened internal tangential wall and a dense cytoplasm with numerous polyribosomes and dictyosomes. (e) Detail of the inner tangential cell walls with an outer layer and an inner layer. Abbreviations: Au, autophagosome; CC, canal cell; CM, cellular membrane; CW, cellular wall; Di, dictyosome; EM, electron-dense material; GM, granular material; ICW, internal cell wall; ILCW, inner layer cell wall; OLCW, outer layer cell wall; M, mitochondria; N, nucleus; Nu, nucleolus; PRI, polyribosome; S, starch; SD, stylar duct; SS, secretion space; StT, stigmatoid tissue; SV, secretion vesicle; TC, thin cuticle; V, vacuole.

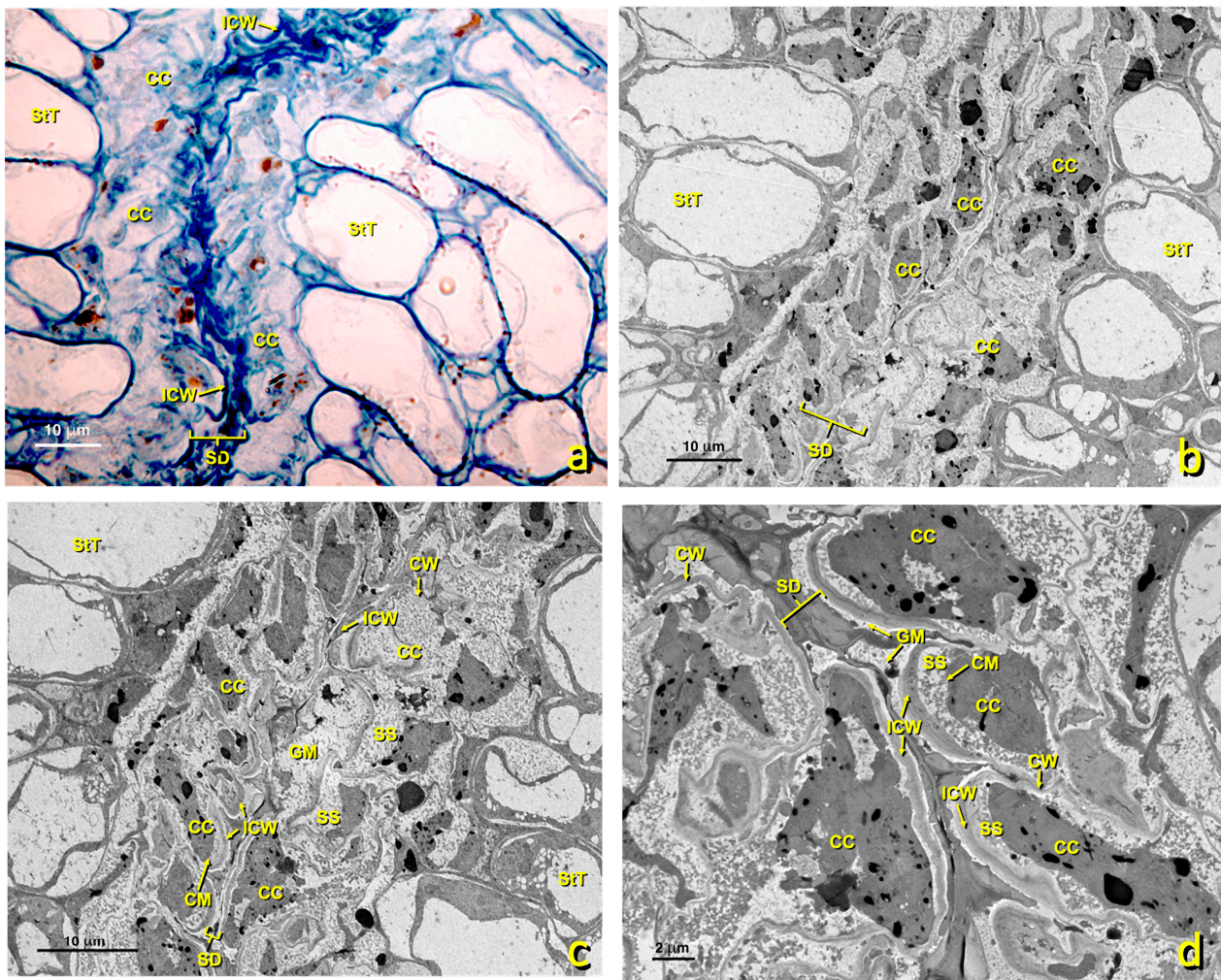


Figure 11. Stylar canal from flowers with a treated stigma. Micrographs of the longitudinal sections of affected stylar canal cells. (a) Micrograph of a semithin section stained with toluidine blue. Canal cells are considerably affected. Bar: 10 μm . (b,c) TEM micrographs of the affected stylar canals at different magnifications. (b) bar 10 μm ; (c) bar 10 μm ; (d) bar 2 μm . Abbreviations: CC, canal cell; CM, cellular membrane; CW, cellular wall; GM, granular material; ICW, internal cell wall; SD, stylar duct; SS, secretion space; StT, stigmatoid tissue.

3.8. Outcome for Other Citrus Species

The stigmas of various *Citrus* species and varieties were treated with sulfur to see if the same effect was observed as on the Nadorcott mandarin stigmas (Figure S2). The sections made by freezing, stained with aniline blue, and viewed by EFM gave the same results as those obtained for Nadorcott. The control flowers (only pollinated) of Clemenules (*Citrus clementina* hort. ex Tanaka; Figure S2a), Clementina Fina (*Citrus clementina* hort. ex Tanaka; Figure S2c), Murcott (*Citrus reticulata* Blanco; Figure S2e), Nova (*C. clementina* \times [*C. paradisi* \times *C. tangerina*]; Figure S2g), Arrufatina (*Citrus clementina* hort. ex Tanaka; Figure S2i) and Lemon Verna (*Citrus limon* (L.) Burm.f.; Figure S2k) showed pollen tube growth inside the stigma, while the sections of the pollinated flowers treated with sulfur displayed no pollen tube development inside the stigma (Figure S2b,d,f,h,j,l).

3.9. Preliminary Outcomes of Other Horticultural Species

Preliminary evidence for the effect of sulfur on the flowers of other horticulture species was obtained. Seeds were found in cucumber (*Cucumis sativus* L.) and eggplant (*Solanum melongena* L.) from the control flowers that were only pollinated (Figure S3a,c),

while no seeds were seen in the fruit from the cucumber and eggplant flowers treated with sulfur and then pollinated (Figure S3b,d). The melon fruit from the sulfur-treated flowers showed asymmetric seed formation, while the melon fruit from the control flowers displayed uniform seed distribution (Figure S3e,f). The control flower sections of eggplant (Figure S3g) and watermelon (*Citrullus lanatus* (Thunb.) Matsumara & Nakai; Figure S3i) showed pollen tube growth inside the stigma, while the sections of the sulfur-treated pollinated flowers revealed no pollen tube development inside the stigma (Figure S3h,j).

4. Discussion

The Nadorcott stigma ultrastructure is similar to that previously described for other citrus [32,33,78]. Nadorcott mandarin presents a wet-type stigma with abundant exudate that uniformly covers the upper papillae, which also occurs in wet-type stigma species [27,28]. This exudate is essential for correct pollen grain adhesion and their subsequent germination. As described for *Citrus × limon* [33] and *Citrus caroliniana* [69], the stigmatic glandular area is arranged in two regions: one made up of elongated papillary cells and another of basal papillary cells.

Cellular tissues have been studied and described in depth, and have provided considerable knowledge of the ultrastructure of both the stigma and style of Nadorcott mandarin, especially of the organelles related to the production of energy and to the synthesis of protein, polysaccharide and lipid substances, mainly mitochondria, dictyosomes and the RER. Abundant RER cisterns allow the existence of plasmodesmata and, therefore, the cellular exchange of protein and other synthetic elements. This extensive knowledge provides a better understanding of the fertilization process. Stylar canals play an important role in the recognition and nutrition of pollen tubes by allowing heterotrophic growth toward the ovule [42,51,52,58]. Proof of this is the complexity displayed by the stylar canals of Nadorcott flowers, where several specialized layers and secreted vesicles have been identified and described. Most of the secreted material found in the stylar canal was amorphous, low electron dense and granular, presumably polysaccharide (according to the results of Ciampolini et al. [32]).

Previous studies have demonstrated that sulfur is very effective in preventing pollen tube growth inside the stigma [72]. This effect was clearly seen when both the sulfur-treated and untreated flowers were compared to epifluorescence UV sections (Figure 2; [72]). This growth inhibition prevents ovule fertilization and, therefore, seed formation in Nadorcott mandarin [73]. Previously, other substances have been tested to prevent seed formation in mandarin and other species, but with poor results [71,79,80].

By studying the treated and untreated flowers (Figures 3–11), pollen tube growth inhibition was caused by the alteration to stigmatic tissues. The upper papillae completely collapsed with severe protoplast disorganization; the basal papillae and stigmatic tissue also showed some disturbed cells, with protoplast collapse and organelle disorganization; even stylar canals were strongly affected. In addition, the treated flowers showed an alteration to and the irregular distribution of the exudate. The TEM observations of the treated stigmas indicated a marked alteration and degradation of numerous cellular organelles. The presence of RER tubules, dictyosomes and polyribosomes was barely appreciated in these affected cells (Figure 6e). The number of secretion vesicles from dictyosomes dropped, which suggests the alteration of these organelles. In addition, the marked decrease in the number of mitochondria could be the cause of the accumulation of lipid bodies, which would not undergo beta oxidation because the substances to be metabolized decreased. In the untreated flowers, the abundant cisterns allowed plasmodesmata to exist and, therefore, the cellular exchange of protein and other synthetic elements, which did not occur in the treated ones.

Pollen grains were observed on the stigma surface of both the treated and untreated flowers, which implied that forced pollination worked. Furthermore, pollen grain germination also occurred in both cases, but in the treated flowers, pollen tubes could not grow toward the inner part of the stigma. All these pieces of evidence suggest that the main effect

of sulfur to prevent fertilization occurs in female tissues. The alteration of stigma tissues does not allow pollen tubes to develop through them. Notwithstanding, some studies have already suggested that sulfur can also have some effect on pollen grain germination [81].

In some treated flowers, affected and unaffected areas were noted (Figure 3), which revealed contact sulfur action that did not extend to other contiguous flower areas.

Preliminary results in other citrus and other horticultural species point to a non-species-specific action. No pollen tubes were observed inside the stigma of the treated flowers of several citrus varieties and horticultural species belonging to Solanaceae and Cucurbitaceae. Asymmetric seed formation in the melon fruit from the sulfur-treated flowers is probably related to its complex and intricate lobed stigma (Figure S3e). In this case, sulfur treatment likely affected the outermost lobes of the flower stigma, which did not set seeds, and did not reach the innermost lobes where seeds formed. This evidence reveals, once more, a generic and contact action of sulfur on stigma tissues, with a marked alteration to the glandular area.

5. Conclusions

Sulfur prevented pollen tube growth inside the stigma of several species and, therefore, prevented ovule fertilization and seed formation. When comparing the treated and untreated flowers, sulfur specifically caused the alteration of the outer layer of stigma papillary cells. This alteration led papillary cells to lose their functionality because their cellular structure deteriorated and degraded, which prevented pollen tubes developing inside the stigma. Basal papillae, stigmatic tissue and stylar canals also underwent alteration. Additionally, sulfur modified both the quantity and uniformity of the distribution of the stigmatic exudate on the stigma surface. These effects were observed in several species and varieties of *Citrus* and some other horticultural species with the same results, which points out generic (non species-specific) action.

6. Patents

The results reported in this study are protected for the international patent application PCT/ES2019/070509.

Supplementary Materials: The following supporting information can be downloaded at: <https://www.mdpi.com/article/10.3390/agronomy13061643/s1>, Figure S1: Pollen tubes growth at the stigmatic area; Figure S2: Results in other *Citrus* ssp.; Figure S3: Preliminary outcomes of several horticultural species.

Author Contributions: Conceptualization, F.G.-B., J.R., A.G. and H.M.; methodology, F.G.-B., J.R., N.C. and R.B.; software, F.G.-B.; validation, F.G.-B., J.R. and H.M.; formal analysis, F.G.-B., J.R., R.B. and N.C.; investigation, F.G.-B., J.R., N.C., C.Z. and R.B.; resources, F.G.-B., J.R. and H.M.; data curation, F.G.-B., J.R., A.G. and H.M.; writing—original draft preparation, F.G.-B., J.R. and H.M.; writing—review and editing, F.G.-B., J.R. and H.M.; visualization, F.G.-B. and H.M.; supervision, F.G.-B., J.R. and H.M.; project administration, H.M.; funding acquisition, H.M. All authors have read and agreed to the published version of the manuscript.

Funding: This research was funded by Asociación Club de Variedades Vegetales Protegidas (<https://www.clubvvp.com/>, accessed on 17 March 2021) as part of a project undertaken with the Universitat Politècnica de València (Spain, UPV 20170087), of which H. Merle was the principal researcher. There was no additional external funding received for this study.

Data Availability Statement: Not applicable.

Acknowledgments: The authors thank the SAEAS farm for providing technical assistance and for access to the orchard.

Conflicts of Interest: The authors declare no conflict of interest.

References

1. Heslop-Harrison, J. Male Gametophyte Selection and the Pollen-Stigma Interaction. In *Gamete Competition in Plants and Animals*; Mulcahy, D.L., Ed.; North Holland: Amsterdam, The Netherlands, 1975; pp. 177–190.
2. Heslop-Harrison, J.; Heslop-Harrison, Y.; Barber, J. The Stigma Surface in Incompatibility Responses. *Proc. R. Soc. London Ser. B. Biol. Sci.* **1975**, *188*, 287–297. [[CrossRef](#)]
3. Gaude, T.; McCormick, S. Signaling in Pollen-Pistil Interactions. *Semin. Cell Dev. Biol.* **1999**, *10*, 139–147. [[CrossRef](#)] [[PubMed](#)]
4. Acosta, M.G.; Lassaga, S.L.; Casco, V.H. Estudio y Caracterización de La Naturaleza Química de La Adhesión Celular Polen-Estigma En *Arabidopsis thaliana*. *Rev. Científica Agropecu.* **2007**, *11*, 141–147.
5. Linskens, H.F. Recognition during the Progametic Phase. In *Biology of Reproduction and Cell Motility in Plants and Animals*; Cresti, M., Dallai, R., Eds.; University of Siena: Siena, Italy, 1986; pp. 21–32.
6. Cheung, A.Y. Pollen-Pistil Interactions during Pollen-Tube Growth. *Trends Plant Sci.* **1996**, *1*, 45–51. [[CrossRef](#)]
7. Gotelli, M.M.; Lattar, E.C.; Zini, L.M.; Galati, B.G. Style Morphology and Pollen Tube Pathway. *Plant Reprod.* **2017**, *30*, 155–170. [[CrossRef](#)] [[PubMed](#)]
8. Bell, P.R. Incompatibility in Flowering Plants: Adaptation of an Ancient Response. *Plant Cell* **1995**, *7*, 5–16. [[CrossRef](#)]
9. Herrero, M.; Hormaza, J.I. Pistil Strategies Controlling Pollen Tube Growth. *Sex. Plant Reprod.* **1996**, *9*, 343–347. [[CrossRef](#)]
10. Sage, T.L.; Hristova-Sarkovski, K.; Koehl, V.; Lyew, J.; Pontieri, V.; Bernhardt, P.; Weston, P.; Bagha, S.; Chiu, G. Transmitting Tissue Architecture in Basal-Relictual Angiosperms: Implications for Transmitting Tissue Origins. *Am. J. Bot.* **2009**, *96*, 183–206. [[CrossRef](#)]
11. Williams, J.H.; Mcneilage, R.T.; Lettre, M.T.; Taylor, M.L. Pollen Tube Growth and the Pollen-Tube Pathway of *Nymphaea odorata* (Nymphaeaceae). *Bot. J. Linn. Soc.* **2010**, *162*, 581–593. [[CrossRef](#)]
12. Endress, P.K.; Igersheim, A. Gynoecium Structure and Evolution in Basal Angiosperms. *Int. J. Plant Sci.* **2000**, *161*, S211–S213. [[CrossRef](#)]
13. Williams, J.H. *Amborella trichopoda* (Amborellaceae) and the Evolutionary Developmental Origins of the Angiosperm Progametic Phase. *Am. J. Bot.* **2009**, *96*, 144–165. [[CrossRef](#)] [[PubMed](#)]
14. Endress, P.K. Angiosperm Ovules: Diversity, Development, Evolution. *Ann. Bot.* **2011**, *107*, 1465–1489. [[CrossRef](#)] [[PubMed](#)]
15. Endress, P.K. Patterns of Angiospermy Development before Carpel Sealing across Living Angiosperms: Diversity, and Morphological and Systematic Aspects. *Bot. J. Linn. Soc.* **2015**, *178*, 556–591. [[CrossRef](#)]
16. Endress, P.K. Syncarpy and Alternative Modes of Escaping Disadvantages of Apocarpy in Primitive Angiosperms. *Taxon* **1982**, *31*, 48–52. [[CrossRef](#)]
17. Ferreira, J.A.B.; Ledo, C.A.S.; Souza, F.V.D.; Conceição, J.Q.; Rossi, M.L.; Souza, E.H. Stigma Structure and Receptivity in Papaya (*Carica papaya* L.). *Acad. Bras. Cienc.* **2021**, *93*, 20190605. [[CrossRef](#)] [[PubMed](#)]
18. Souza, E.H.; Carmello-Guerreiro, S.M.; Souza, F.V.D.; Rossi, M.L.; Martinelli, A.P. Stigma Structure and Receptivity in Bromeliaceae. *Sci. Hortic.* **2016**, *203*, 118–125. [[CrossRef](#)]
19. Teixeira, S.P.; Costa, M.F.B.; Basso-Alves, J.P.; Kjellberg, F.; Pereira, R.A.S. Morphological Diversity and Function of the Stigma in *Ficus* Species (Moraceae). *Acta Oecologica.* **2018**, *90*, 117–131. [[CrossRef](#)]
20. Heslop-Harrison, J.; Heslop-Harrison, Y. The Pollen-Stigma Interaction in the Grasses. I. Fine-Structure and Cytochemistry of the Stigmas of *Hordeum* and *Secale*. *Acta Bot. Neerl.* **1980**, *29*, 261–276. [[CrossRef](#)]
21. Linskens, H.F.; Heinen, W. Cutinase-Nachweis in Pollen. *Z. Bot.* **1962**, *50*, 338–347.
22. Mattsson, O.; Knox, R.B.; Heslop-Harrison, J.; Heslop-Harrison, Y. Protein Pellicle of Stigmatic Papillae as a Probable Recognition Site in Incompatibility Reactions. *Nature* **1974**, *247*, 298–300. [[CrossRef](#)]
23. Safavian, D.; Goring, D.R. Secretory Activity is Rapidly Induced in Stigmatic Papillae by Compatible Pollen, but Inhibited for Self-Incompatible Pollen in the Brassicaceae. *PLoS ONE* **2013**, *8*, e84286. [[CrossRef](#)] [[PubMed](#)]
24. Heslop-Harrison, Y.; Shivanna, K.R. The Receptive Surface of the Angiosperm Stigma. *Ann. Bot.* **1977**, *41*, 1233–1258. [[CrossRef](#)]
25. Katano, K.; Suzuki, N. What Are the Key Mechanisms That Alter the Morphology of Stigmatic Papillae in *Arabidopsis thaliana*? *Plant Signal. Behav.* **2021**, *16*, 1980999. [[CrossRef](#)] [[PubMed](#)]
26. Lu, X.; Ye, X.; Hu, Z.; Liu, J. The Morphology of Stigma of Asteraceae Observed by Scanning Electron Microscopy. *Microsc. Res. Tech.* **2022**, *85*, 2292–2304. [[CrossRef](#)] [[PubMed](#)]
27. Jordaan, A.; Wessels, D.C.J.; Krüger, H. Structure of the Style and Wet Non-Papillate Stigma of *Colophospermum mopane*, Caesalpinioideae: *Detarieae*. *Bot. J. Linn. Soc.* **2002**, *139*, 295–304. [[CrossRef](#)]
28. Owens, S.J. The Morphology of the Wet, Non-Papillate (WN) Stigma Form in the Tribe Caesalpinieae (Caesalpinioideae: Leguminosae). *Bot. J. Linn. Soc.* **1990**, *104*, 293–302. [[CrossRef](#)]
29. Slater, A.T.; Calder, D.M. Fine Structure of the Wet, Detached Cell Stigma of the Orchid *Dendrobium speciosum* Sm. *Sex. Plant Reprod.* **1990**, *3*, 61–69. [[CrossRef](#)]
30. Shivanna, K.R.; Sastri, D.C. Stigma-Surface Esterase Activity and Stigma Receptivity in Some Taxa Characterized by Wet Stigmas. *Ann. Bot.* **1981**, *47*, 53–64. [[CrossRef](#)]
31. de Nettancourt, D. *Incompatibility in Angiosperms*; Springer: Berlin/Heidelberg, Germany, 1977. [[CrossRef](#)]
32. Ciampolini, F.; Cresti, M.; Sarfatti, G.; Tiezzi, A. Ultrastructure of the Stylar Canal Cells of *Citrus limon* (Rutaceae). *Plant Syst. Evol.* **1981**, *138*, 263–274. [[CrossRef](#)]

33. Cresti, M.; Ciampolini, F.; van Went, J.L.; Wilms, H.J. Ultrastructure and Histochemistry of *Citrus limon* (L.) Stigma. *Planta* **1982**, *156*, 1–9. [[CrossRef](#)]
34. Distefano, G.; Gentile, A.; Herrero, M. Pollen-Pistil Interactions and Early Fruiting in Parthenocarpic Citrus. *Ann. Bot.* **2011**, *108*, 499–509. [[CrossRef](#)]
35. Edlund, A.F.; Swanson, R.; Preuss, D. Pollen and Stigma Structure and Function: The Role of Diversity in Pollination. *Plant Cell* **2004**, *16*, S84–S97. [[CrossRef](#)]
36. Graaf, B.H.J.D.; Derksen, J.W.M.; Mariani, C. Pollen and Pistil in the Progametic Phase. *Sex. Plant Reprod.* **2001**, *14*, 41–55. [[CrossRef](#)]
37. Swanson, R.; Edlund, A.F.; Preuss, D. Species Specificity in Pollen-Pistil Interactions. *Annu. Rev. Genet.* **2004**, *38*, 793–818. [[CrossRef](#)]
38. Ciampolini, F.; Cresti, M.; Kapil, R.N.; Crest, M. Fine Structural and Cytochemical Characteristics of Style and Stigma in Olive. *Caryologia* **1983**, *36*, 211–230. [[CrossRef](#)]
39. Bigazzi, M.; Selvi, F. Stigma Form and Surface in the Tribe Boragineae (Boraginaceae): Micromorphological Diversity, Relationships with Pollen, and Systematic Relevance. *Can. J. Bot.* **2000**, *78*, 388–408.
40. Herrero, M.; Dickinson, H.G. Pollen-Pistil Incompatibility in *Petunia hybrida*: Changes in the Pistil Following Compatible and Incompatible Intraspecific Crosses. *J. Cell Sci.* **1979**, *36*, 1–18. [[CrossRef](#)]
41. Labarca, C.; Loewus, F. The Nutritional Role of Pistil Exudate in Pollen Tube Wall Formation in *Lilium longiflorum*: II. Production and Utilization of Exudate from Stigma and Stylar Canal. *Plant Physiol.* **1973**, *52*, 87–92. [[CrossRef](#)] [[PubMed](#)]
42. Herrero, M.; Dickinson, H.G. Pollen Tube Development in *Petunia hybrida* Following Compatible and Incompatible Intraspecific Matings. *J. Cell Sci.* **1981**, *47*, 365–383. [[CrossRef](#)]
43. Stephenson, A.G.; Travers, S.E.; Mena-Ali, J.I.; Winsor, J.A. Pollen Performance before and during the Autotrophic-Heterotrophic Transition of Pollen Tube Growth. *Philos. Trans. R. Soc. London. Ser. B Biol. Sci.* **2003**, *358*, 1009–1018. [[CrossRef](#)] [[PubMed](#)]
44. Sassen, M.M.A. The Stylar Transmitting Tissue. *Acta Bot. Neerl.* **1974**, *23*, 99–108. [[CrossRef](#)]
45. Lennon, K.A.; Roy, S.; Hepler, P.K.; Lord, E.M. The Structure of the Transmitting Tissue of *Arabidopsis thaliana* (L.) and the Path of Pollen Tube Growth. *Sex. Plant Reprod.* **1998**, *11*, 49–59. [[CrossRef](#)]
46. Knox, R.B. Pollen—Pistil interaction. In *Encyclopedia Plant Physiology*; Linskens, H.F., Heslop-Harrison, J., Eds.; Cellular Interactions; Springer: Berlin/Heidelberg, Germany; New York, NY, USA; Tokyo, Japan, 1984; pp. 508–608.
47. Heslop-Harrison, J. Pollen Germination and Pollen-Tube Growth. *Int. Rev. Cytol.* **1987**, *107*, 1–78. [[CrossRef](#)]
48. Wu, H.M.; Wang, H.; Cheung, A.Y. A Pollen Tube Growth Stimulatory Glycoprotein Is Deglycosylated by Pollen Tubes and Displays a Glycosylation Gradient in the Flower. *Cell* **1995**, *82*, 395–403. [[CrossRef](#)]
49. Jauh, G.Y.; Lord, E.M. Movement of the Tube Cell in the Lily Style in the Absence of the Pollen Grain and the Spent Pollen Tube. *Sex. Plant Reprod.* **1995**, *8*, 168–172. [[CrossRef](#)]
50. Wilhelmi, L.K.; Preuss, D. Self-Sterility in *Arabidopsis* Due to Defective Pollen Tube Guidance. *Science* **1996**, *274*, 1535–1537. [[CrossRef](#)]
51. Wilhelmi, L.K.; Preuss, D. The Mating Game: Pollination and Fertilization in Flowering Plants. *Curr. Opin. Plant Biol.* **1999**, *2*, 18–22. [[CrossRef](#)] [[PubMed](#)]
52. Shimizu, K.K.; Okada, K. Attractive and Repulsive Interactions between Female and Male Gametophytes in *Arabidopsis* Pollen Tube Guidance. *Development* **2000**, *127*, 4511–4518. [[CrossRef](#)] [[PubMed](#)]
53. Hudák, J.; Walles, B.; Vennigerholz, F. The Transmitting Tissue in *Brugmansia suaveolens* L.: Ultrastructure of the Stylar Transmitting Tissue. *Ann. Bot.* **1993**, *71*, 177–186. [[CrossRef](#)]
54. Wilhelmi, L.K.; Preuss, D. Blazing New Trails (Pollen Tube Guidance in Flowering Plants). *Plant Physiol.* **1997**, *113*, 307–312. [[CrossRef](#)] [[PubMed](#)]
55. Jauh, G.Y.; Eckard, K.J.; Nothnagel, E.A.; Lord, E.M. Adhesion of Lily Pollen Tubes on an Artificial Matrix. *Sex. Plant Reprod.* **1997**, *10*, 173–180. [[CrossRef](#)]
56. Vennigerholz, F. The Transmitting Tissue in *Brugmansia suaveolens*: Immunocytochemical Localization of Pectin in the Style. *Protoplasma* **1992**, *171*, 117–122. [[CrossRef](#)]
57. Malhó, R. Pollen Tube Guidance—The Long and Winding Road. *Sex. Plant Reprod.* **1998**, *11*, 242–244. [[CrossRef](#)]
58. Lind, J.L.; Böning, I.; Clarke, A.E.; Anderson, M.A. A Style-Specific 120-KDa Glycoprotein Enters Pollen Tubes of *Nicotiana glauca* in Vivo. *Sex. Plant Reprod.* **1996**, *9*, 75–86. [[CrossRef](#)]
59. Kroh, M.; Miki-Hirosige, H.; Rosen, W.; Loewus, F. Incorporation of Label into Pollen Tube Walls from Myo-inositol-Labeled *Lilium longiflorum* Pistils. *Plant Physiol.* **1970**, *45*, 92–94. [[CrossRef](#)]
60. Rosen, W.G.; Thomas, H.R. Secretory Cells of Lily pistils. I. Fine structure and Function. *Am. J. Bot.* **1970**, *57*, 1108–1114. [[CrossRef](#)]
61. Vasilev, A.E. Ultrastructure of Stigmatoid Cells in *Lilium*. *Sov Plant Physiol* **1970**, *17*, 1035–1044.
62. Clarke, A.E.; Considine, J.A.; Ward, R.; Knox, R.B. Mechanism of Pollination in *Gladiolus*: Roles of Stigma and Pollen Tube Guide. *Ann. Bot.* **1977**, *41*, 15–20. [[CrossRef](#)]
63. Tilton, V.R.; Horner, H.T. Stigma, Style, and Obturator of *Ornithogalum caudatum* (Liliaceae) and Their Function in the Reproductive Process. *Am. J. Bot.* **1980**, *67*, 1113–1131. [[CrossRef](#)]
64. Owens, S.J.; Mcgrath, S.; Fraser, M.A.; Fox, L.R. The Anatomy, Histochemistry and Ultrastructure of Stigmas and Styles in Commelinaceae. *Ann. Bot.* **1984**, *54*, 591–603. [[CrossRef](#)]

65. Lord, E.M.; Kohorn, L.U. Gynoecial Development, Pollination, and the Path of Pollen Tube Growth in the Tepary Bean, *Phaseolus acutifolius*. *Am. J. Bot.* **1986**, *73*, 70–78. [[CrossRef](#)]
66. Leins, P.; Erbar, C. Floral Morphological Studies in the South African *Cyphia stenopetala* Diels (Cyphiaceae). *Int. J. Plant Sci.* **2005**, *166*, 207–217. [[CrossRef](#)]
67. Reinhardt, S.; Ewalda, A.; Hellwig, F. The Anatomy of the Stigma and Style from *Cyclamen persicum* (Mill.) Cv. “Pure White” and Its Relation to Pollination Success. *Plant Biol.* **2007**, *9*, 158–162. [[CrossRef](#)] [[PubMed](#)]
68. Castro, S.; Silva, S.; Stanesco, I.; Silveira, P.; Navarro, L.; Santos, C. Pistil Anatomy and Pollen Tube Development in Polygala Vayredae Costa (Polygalaceae). *Plant Biol.* **2009**, *11*, 405–416. [[CrossRef](#)]
69. Galati, B.G.; Rosenfeldt, S.; Zarlavsky, G.; Gotelli, M.M. Ultrastructure of the Stigma and Style of *Cabomba caroliniana* Gray (Cabombaceae). *Protoplasma* **2016**, *253*, 155–162. [[CrossRef](#)]
70. Gotelli, M.M.; Galati, B.G.; Medan, D. Structure of the Stigma and Style in *Colletia* and *Discaria* (Rhamnaceae: Colletieae). *Plant Syst. Evol.* **2012**, *298*, 1635–1641. [[CrossRef](#)]
71. Garmendia, A.; Beltrán, R.; Zornoza, C.; Breijo, F.; Reig, J.; Bayona, I.; Merle, H. Insect Repellent and Chemical Agronomic Treatments to Reduce Seed Number in ‘Afourer’ Mandarin. Effect on Yield and Fruit Diameter. *Sci. Hortic.* **2019**, *246*, 437–447. [[CrossRef](#)]
72. Garmendia, A.; García-Breijo, F.; Reig, J.; Raigón, M.D.; Beltrán, R.; Zornoza, C.; Cebrián, N.; Merle, H. Agronomic Treatments to Avoid Seed Presence in ‘Nadorcott’ Mandarin I. Effect on in Vivo Pollen Tube Growth. *Sci. Hortic.* **2022**, *294*, 110760. [[CrossRef](#)]
73. Garmendia, A.; Raigón, M.D.; García-Breijo, F.; Reig, J.; Beltrán, R.; Zornoza, C.; Cebrián, N.; Merle, H. Agronomic Treatments to Avoid Presence of Seeds in Nadorcott Mandarin II. Effect on Seed Number per Fruit and Yield. *PLoS ONE* **2022**, *17*, e0278934. [[CrossRef](#)] [[PubMed](#)]
74. Nadori, E.B. Mandarin Tangerine Called Nadorcott. U.S. Patent 10,480, 7 July 1998.
75. Morris, J.K. A Formaldehyde Glutaraldehyde Fixative of High Osmolality for Use in Electron Microscopy. *J. Cell Biol.* **1965**, *27*, 1A–149A.
76. Molins, A.; Moya, P.; García-Breijo, F.J.; Reig-Armiñana, J.; Barreno, E. A Multi-Tool Approach to Assess Microalgal Diversity in Lichens: Isolation, Sanger Sequencing, HTS and Ultrastructural Correlations. *Lichenologist* **2018**, *50*, 123–138. [[CrossRef](#)]
77. Ruzin, S.E. *Plant Microtechnique and Microscopy*; Oxford University Press: New York, NY, USA, 1999.
78. Wetzstein, H.Y.; Law, S.E. Enhanced Visualization of the Fine Structure of the Stigmatic Surface of *Citrus* Using Pre-Fixation Washes. *J. Am. Soc. Hortic. Sci.* **2012**, *137*, 290–293. [[CrossRef](#)]
79. Gambetta, G.; Gravina, A.; Fasiolo, C.; Fornero, C.; Galiger, S.; Inzaurrealde, C.; Rey, F. Self-Incompatibility, Parthenocarpy and Reduction of Seed Presence in “Afourer” Mandarin. *Sci. Hortic.* **2013**, *164*, 183–188. [[CrossRef](#)]
80. Gonzatto, M.P.; Griebeler, S.R.; de Almeida, G.K.; Munhoz, B.d.O.; Sulzbach, M.; Schwarz, S.F. Parthenocarpy Induction and Reduction of Seeds in Fruits of Nadorcott’ mandarin. *Rev. Ceres* **2022**, *69*, 167–172. [[CrossRef](#)]
81. Beltrán, R.; Cebrián, N.; Zornoza, C.; Breijo, F.G.; Armiñana, J.R.; Garmendia, A.; Merle, H. Effect of Sulfur on Pollen Germination of Clemenules Mandarin and Nova Tangelo. *PeerJ* **2023**, *11*, e14775. [[CrossRef](#)]

Disclaimer/Publisher’s Note: The statements, opinions and data contained in all publications are solely those of the individual author(s) and contributor(s) and not of MDPI and/or the editor(s). MDPI and/or the editor(s) disclaim responsibility for any injury to people or property resulting from any ideas, methods, instructions or products referred to in the content.